PERGAMON

Vision Research 40 (2000) 1711–1737

Vision Research

www.elsevier.com/locate/visres

The spectral sensitivities of the middle- and long-wavelength-sensitive cones derived from measurements in observers of known genotype

Andrew Stockman [a,*], Lindsay T. Sharpe [b]

[a] *Department of Psychology 0109, University of California San Diego, 9500 Gilman Drive, La Jolla, CA 92093-0109, USA*
[b] *Forschungsstelle für Experimentelle Ophthalmologie, Röntgenweg 11, D-72076 Tübingen, Germany*

Received 15 August 1998; received in revised form 5 January 2000

Abstract

The spectral sensitivities of middle- (M-) and long- (L-) wavelength-sensitive cones have been measured in dichromats of known genotype: M-cone sensitivities in nine protanopes, and L-cone sensitivities in 20 deuteranopes. We have used these dichromat cone spectral sensitivities, along with new luminous efficiency determinations, and existing spectral sensitivity and color matching data from normal trichromats, to derive estimates of the human M- and L-cone spectral sensitivities for 2 and 10° dia. central targets, and an estimate of the photopic luminosity function [$V(\lambda)$] for 2° dia. targets, which we refer to as $V_2^*(\lambda)$. These new estimates are consistent with dichromatic and trichromatic spectral sensitivities and color matches.

Keywords: M-cones; L-cones; Spectral sensitivity; Cone fundamentals; Molecular genetics; Photopigments; Photopigment genes; Macular pigment; Lens pigment; Color matching; Single-gene dichromats; Dichromacy; Protanopes; Deuteranopes

1. Introduction

The three types of cone photoreceptors, each with different spectral sensitivity, are the foundations of our trichromatic color vision. They are referred to as long-, middle- and short-wavelength-sensitive (L, M and S), according to the relative spectral positions of their peak sensitivities. In this paper, we derive new estimates of the M- and L-cone spectral sensitivities (or cone 'fundamentals') based on the fits of color matching data to M- and L-cone spectral sensitivity measurements obtained in nine protanopes and 20 deuteranopes of known genotype (Sharpe, Stockman, Jägle, Knau, Klausen, Reitner et al., 1998a). The color matching data that we used were the color matching functions (CMFs) for the central 2° of vision obtained by Stiles and Burch (Stiles, 1955) and the 10° CMFs obtained by Stiles and Burch (1959); the latter are retabulated in Table 3 of Appendix A. We also consider new tritanopic color matching data (Stockman & Sharpe, 2000) and existing spectral sensitivity data from normals (Stockman, MacLeod & Johnson, 1993a), as well as new luminous efficiency measurements in normals. This work complements a recent estimate of S-cone spectral sensitivity by Stockman, Sharpe and Fach (1999), which is also tabulated in Table 2. In the following sections, we introduce cone spectral sensitivity measurements and discuss the relationship between such measurements and color matching data. A brief outline of the relevant molecular genetics is also provided.

1.1. L- and M-cone spectral sensitivity measurements

The spectral sensitivities of the three cone types overlap extensively throughout the spectrum. Consequently, the measurement of the spectral sensitivity of a single cone type in the normal trichromatic observer requires special procedures to isolate its response from the responses of the other two unwanted cone types.

* Corresponding author. Tel.: +1-858-534-4762; fax: +1-858-534-7190.
E-mail address: astockman@ucsd.edu (A. Stockman)

0042-6989/00/$ - see front matter
PII: S0042-6989(00)00021-3

Most isolation techniques are variations of the two-color threshold technique of W.S. Stiles (Stiles, 1939, 1978), so-called because the detection threshold for a target or test field of one wavelength is measured on a larger adapting or background field usually of a second wavelength (or mixture of wavelengths). In Stiles' 'test' sensitivity measurements, a variation of which was used in the following work, the background field is fixed at a wavelength that selectively suppresses the sensitivities of two unwanted cone types, but spares the one of interest. Spectral sensitivity is then determined by measuring the target radiance required to detect some feature of the target as a function of its wavelength.

If, as in this work, target detection mediated by the S-cones must be prevented, S-cone sensitivity can be further impaired by the use of targets of high temporal and/or spatial frequencies, to which the S-cone visual pathways are relatively insensitive (e.g. Stiles, 1949; Brindley, 1954; Brindley, Du Croz & Rushton, 1966). The use of moderate to high frequency heterochromatic flicker photometry (HFP, see Section 2), in particular, is thought to eliminate or at least reduce any S-cone contribution (e.g. Eisner & MacLeod, 1980; but see Stockman, MacLeod & DePriest, 1991). Using such tasks, the isolation of the M- and L-cone responses from the S-cone response is fairly straightforward. The isolation of the M- and L-cone responses from each other is more difficult, however.

1.1.1. L- and M-cone measurements in normals

There have been several attempts to measure complete M- and L-cone spectral sensitivities in normals using variations of the test sensitivity method (e.g. Wald, 1964; Eisner & MacLeod, 1981; Stockman & Mollon, 1986; Stockman et al., 1993a). Stiles also made extensive test sensitivity measurements (see, in particular, Stiles, 1964), but explicit in his model of the cone- or π-mechanisms (see, for example, Table 2 (7.4.1) and Table 2 (7.4.3) and Sections 7.4.2 and 7.4.3 of Wyszecki & Stiles, 1982) is the prediction that the test sensitivity method should fail to isolate the M-cone (π_4) response from the L-cone (π_5), and vice versa, in some parts of the visible spectrum.

The separation of the M- from the L-cone responses fails most clearly under 'homochromatic' conditions, when the target is of the same wavelength as the background field, as it must be in any complete spectral sensitivity determination. Under such conditions, the improvement in isolation achieved by the selective desensitization of the unwanted cone type by the background is offset by the insensitivity of the wanted cone type to the target. If the sensitivities of the two cone types are independently set in accordance with Weber's law ($\Delta I/I = k$, where ΔI is the threshold radiance of the target and I is the radiance of the background), as in Stiles' π-mechanism model, the two factors cancel each other completely: the background raises the threshold of the unwanted cone, relative to that of the wanted one, by the *same* amount that the target lowers it. The cone types are then equally sensitive to the target.

Complete cone isolation can be achieved with the test sensitivity method, but only if the selective sensitivity losses due to adaptation by the background *exceed* the selective effect of the target (King-Smith & Webb, 1974; Stockman & Mollon, 1986). Adaptation, in other words, must exceed Weber's law independently for each cone type (see Fig. 2 of Stockman & Mollon, 1986). One way of causing adaptation to exceed Weber's law is to make the adaptation transient. Stockman, MacLeod and Vivien (1993b) found that temporally alternating the adapting field in both color and intensity suppressed the unwanted cone type sufficiently to isolate either the M- or the L-cones throughout the visible spectrum. M-cone spectral sensitivity to a 17-Hz flickering target was measured immediately following the exchange from a blue (485-nm) to a deep-red (678-nm) field, while L-cone spectral sensitivity was measured following the exchange from a deep-red to a blue field (see also King-Smith & Webb, 1974). The field wavelengths were chosen to maximize (or nearly maximize) either the ratio of M- to L-cone excitation (485-nm) or the ratio of L- to M-cone excitation (678-nm). The mean data obtained using this technique by Stockman et al. (1993a) are shown in Fig. 1.

1.1.2. L- or M-cone measurements in X-chromosome-linked dichromats

Cone isolation can be simplified by the use of special observers, who lack one or more of the three cone types. A traditional method of estimating the M- and L-cone spectral sensitivities, and the principal method used here, is to employ X-chromosome-linked dichromats, or, as they are also known, red–green dichromats: protanopes, who are missing L-cone function, and deuteranopes, who are missing M-cone function. If the conditions are chosen so that the S-cones do not contribute to sensitivity (see above), L- or M-cone spectral sensitivity can be measured directly in such observers.

The use of red–green dichromats to define normal-cone spectral sensitivities, however, requires dichromats whose color vision conforms to the 'loss', 'reduction' or 'König' hypothesis: that is, the spectral sensitivity of their surviving M- or L-cone must be identical to that of the corresponding cone type in normal observers (Maxwell, 1856, 1860; König & Dieterici, 1886). We can now be more secure in this assumption, since it is possible to sequence and identify the photopigment genes of normal and dichromat observers (Nathans, Piantanida, Eddy, Shows & Hogness, 1986a; Nathans, Thomas & Hogness, 1986b), and so distinguish those individuals who conform, genetically, to the 'reduction' hypothesis.

For this work, we selected protanopes and deuteranopes who have L- and M-cone photopigment genes that produce 'normal' photopigments. The majority of them have just a single L- or M-cone photopigment gene in the tandem array on the X-chromosome (see Section 1.5, below). In contrast, the protanopes and deuteranopes used in earlier spectral sensitivity studies (e.g. Pitt, 1935; Hecht, 1949; Hsia & Graham, 1957) were of unknown genotype and their X-chromosomes may have carried and expressed hybrid genes that encode for anomalous pigments, or multiple genes that encode pigments with slightly variant spectral sensitivity (see Sharpe et al., 1998a).

1.2. Color matching and cone spectral sensitivities

The trichromacy of individuals with normal color vision is evident in their ability to match any test light to a mixture of three 'primary' lights. The relative intensities of the primary lights required to match equal-energy test lights, λ, are referred to as the red, green and blue[1] color matching functions (CMFs), respectively, and written $\bar{r}(\lambda)$, $\bar{g}(\lambda)$ and $\bar{b}(\lambda)$. If the CMF is negative, the primary light in question must be added to the test field to complete the match.

CMFs can be linearly transformed to other sets of real and imaginary primary lights, such as the X, Y and Z primaries favored by the CIE, or the L, M and S cone fundamental primaries that underlie all trichromatic color matches. Each transformation is accomplished by multiplying the CMFs by a 3×3 matrix. The goal is to determine the unknown 3×3 matrix that will transform the CMFs, $\bar{r}(\lambda)$, $\bar{g}(\lambda)$ and $\bar{b}(\lambda)$, to the three cone spectral sensitivities, $\bar{l}(\lambda)$, $\bar{m}(\lambda)$ and $\bar{s}(\lambda)$.

Color matches are determined at the cone level. When matched, the test and mixture fields appear identical to all three cone classes. Thus, for matched fields, the following relationships apply:

$$\begin{aligned} &\bar{l}_R\bar{r}(\lambda) + \bar{l}_G\bar{g}(\lambda) + \bar{l}_B\bar{b}(\lambda) = \bar{l}(\lambda); \\ &\bar{m}_R\bar{r}(\lambda) + \bar{m}_G\bar{g}(\lambda) + \bar{m}_B\bar{b}(\lambda) = \bar{m}(\lambda); \quad \text{and} \\ &\bar{s}_R\bar{r}(\lambda) + \bar{s}_G\bar{g}(\lambda) + \bar{s}_B\bar{b}(\lambda) = \bar{s}(\lambda) \end{aligned} \tag{1}$$

where $\bar{l}_R$, $\bar{l}_G$ and $\bar{l}_B$ are, respectively, the L-cone sensitivities to the R, G and B primary lights; and similarly, $\bar{m}_R$, $\bar{m}_G$ and $\bar{m}_B$ are the M-cone sensitivities to the primary lights; and $\bar{s}_R$, $\bar{s}_G$ and $\bar{s}_B$ are the S-cone sensitivities. We know $\bar{r}(\lambda)$, $\bar{g}(\lambda)$ and $\bar{b}(\lambda)$, and we assume, for the red R primary, that $\bar{s}_R$ is effectively zero, since the S-cones are insensitive to long-wavelength lights (the intensity of the spectral light λ, which is also known, is equal in energy units throughout the spectrum, and so is discounted from the above equations).

[1] Though the CMFs are referred to as red, green and blue, the actual primary lights that are typically used (e.g. by Stiles, 1955; Stiles & Burch, 1959) appear red, green and violet to the normal observer.

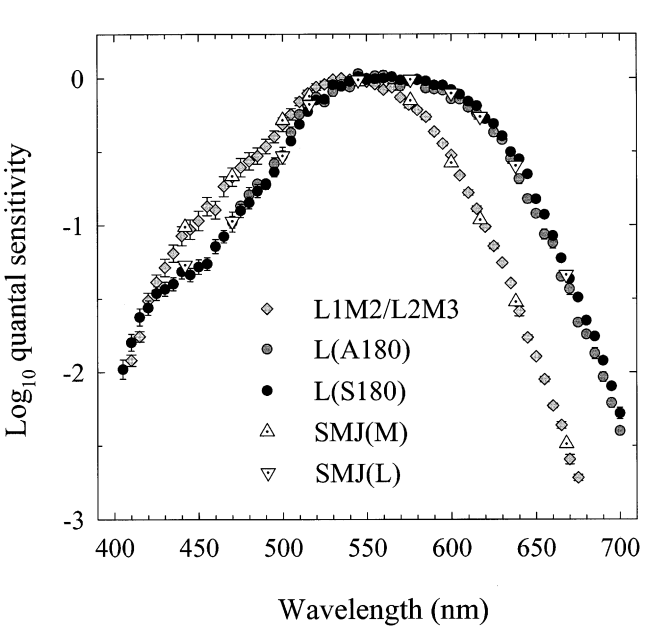

Fig. 1. Comparison of mean spectral sensitivity data. L-cone data for fifteen L(S180) deuteranopes (black circles), five L(A180) deuteranopes (gray circles) and M-cone data for nine protanopes (gray diamonds) from Sharpe et al. (1998a). L-cone data (white dotted inverted triangles) for twelve normals and four deuteranopes and M-cone data (white dotted triangles) for nine normals and two protanopes from Stockman et al. (1993a). Three of the five L(A180) observers made measurements only at wavelengths longer than 470 nm, so the mean data for that group are restricted to that region. The two other means include data only from subjects who made measurements throughout the spectrum.

There are, therefore, only eight unknowns required for the linear transformation:

$$\begin{pmatrix} \bar{l}_R & \bar{l}_G & \bar{l}_B \\ \bar{m}_R & \bar{m}_G & \bar{m}_B \\ 0 & \bar{s}_G & \bar{s}_B \end{pmatrix} \begin{pmatrix} \bar{r}(\lambda) \\ \bar{g}(\lambda) \\ \bar{b}(\lambda) \end{pmatrix} = \begin{pmatrix} \bar{l}(\lambda) \\ \bar{m}(\lambda) \\ \bar{s}(\lambda) \end{pmatrix} \tag{2}$$

However, because we are usually unconcerned about the absolute sizes of $\bar{l}(\lambda)$, $\bar{m}(\lambda)$ and $\bar{s}(\lambda)$, the eight unknowns collapse to just five:

$$\begin{pmatrix} \bar{l}_R/\bar{l}_B & \bar{l}_G/\bar{l}_B & 1 \\ \bar{m}_R/\bar{m}_B & \bar{m}_G/\bar{m}_B & 1 \\ 0 & \bar{s}_G/\bar{s}_B & 1 \end{pmatrix} \begin{pmatrix} \bar{r}(\lambda) \\ \bar{g}(\lambda) \\ \bar{b}(\lambda) \end{pmatrix} = \begin{pmatrix} k_l\,\bar{l}(\lambda) \\ k_m\,\bar{m}(\lambda) \\ k_s\,\bar{s}(\lambda) \end{pmatrix} \tag{3}$$

where the absolute values of k_l(or $1/\bar{l}_B$), k_m(or $1/\bar{m}_B$), and k_s (or $1/\bar{s}_B$) remain unknown, but are typically chosen to scale three functions in some way: for example, so that $k_l\,\bar{l}(\lambda)$, $k_m\,\bar{m}(\lambda)$ and $k_s\,\bar{s}(\lambda)$ peak at unity. In the well-known solution of Eq. (3) by Smith and Pokorny (1975), $k_l\,\bar{l}(\lambda) + k_m\,\bar{m}(\lambda)$ sum to $V(\lambda)$, the luminosity function.

Eqs. (1)–(3) (and Eqs. (4) and (5), below) could be for an equal-energy or an equal-quanta spectrum. Since the CMFs are invariably tabulated for test lights of

equal-energy, we, like previous workers, use an equal-energy spectrum to define the unknowns in the equations and to calculate the cone spectral sensitivities from the CMFs. We then convert the relative cone spectral sensitivities from energy to quantal sensitivities (by multiplying by λ^{-1}). Thus, Table 2, in which the cone fundamentals are tabulated, is in quantal units, whereas Table 3, in which the Stiles and Burch (1959) 10° CMFs are tabulated, is in energy units.

Our aim is to use cone spectral sensitivity measurements to determine the unknowns in Eq. (3) (see also Stockman et al., 1999).

1.3. Color matching data

The validity of Eq. (3) depends not only on determining the correct unknowns, but also on the accuracy of the CMFs themselves. There are several sets of CMFs that could be used to derive cone spectral sensitivities. For the central 2° of vision, the main candidates are the CIE 1931 functions (CIE, 1932), the Judd (1951) and Vos (1978) corrected version of the CIE 1931 functions, and the Stiles and Burch (1955) functions. In addition, the 10° CMFs of Stiles and Burch (1959), or the 10° CIE 1964 CMFs (which are based mainly on the Stiles and Burch (1959), and partly on the Speranskaya (1959) 10° data, see below) can be corrected to correspond to 2° macular and photopigment optical densities.

There are several difficulties associated with the CIE 1931 2° CMFs, and its variants (Judd, 1951; Vos, 1978), not least of which is that they were not directly measured. Instead, they were reconstructed from the relative color matching data of Wright (1928) and Guild (1931) with the assumption that a linear combination of the reconstructed CMFs must equal the 1924 CIE $V(\lambda)$ function. Unfortunately, the validity of the $V(\lambda)$ curve used in the reconstruction is highly questionable (see Gibson & Tyndall, 1923; CIE, 1926; Judd, 1951), as too is the validity of the reconstruction method (Sperling, 1958). The subsequent revisions by Judd (1951) and Vos (1978) are attempts to improve the original $V(\lambda)$. For further discussion, see Stockman and Sharpe (1999).

Color matching functions for 2° vision can be measured directly instead of being constructed by the combination of relative color matching data and photometric data. The Stiles and Burch (1955) 2° CMFs are an example of directly measured functions. With characteristic caution, Stiles referred to these 2° functions as 'pilot' data, yet they are the most extensive set of true CMFs for 2° vision, being based on matches made by ten observers. Given, however, the extent of individual variability that occurs between color normals — the L-cone polymorphism, in particular (see below) — such a small group is unlikely to represent precisely the mean color matches of the normal population.

The most comprehensive set of CMF data, which were also directly measured, are the 'large field' 10° CMFs of Stiles and Burch (1959). Measured in 49 subjects from 392.2 to 714.3 nm (and in nine subjects from 714.3 to 824.2 nm), they are available as individual as well as mean data. During their measurement, the luminance of the matching field was kept high to reduce possible rod intrusion, but nevertheless a small correction for rod intrusion can be applied (see Wyszecki & Stiles, 1982, p. 140).

The large field CIE 1964 CMFs are based mainly on the 10° CMFs of Stiles and Burch (1959), and to a lesser extent on the 10° CMFs of Speranskaya (1959). While the CIE 1964 CMFs are similar to the 10° CMFs of Stiles and Burch (1959), they differ in ways that compromise their use as the basis for cone fundamentals (see also Stockman et al., 1999).

In conclusion, we chose to base our cone fundamentals on the 10° Stiles & Burch CMFs, in accordance with the decisions of the CIE committee (see next section), because they were directly measured in a large group of subjects and because they are relatively uncontaminated by adjustments introduced by other CIE committees. Such changes, though well-intentioned, are often unnecessary and lead to unwanted distortions of the underlying color matching data and cone fundamentals.

1.4. Commission Internationale de l'Éclairage TC 1-36

The analysis described in this paper was motivated in part to furnish new estimates of the cone fundamentals for technical committee, TC 1-36 of the Commission Internationale de l'Éclairage (chairperson: Françoise Viénot; secretary: Pieter Walraven), which has been set the task of defining a 'fundamental chromaticity diagram with physiologically significant axes.' The original cone spectral sensitivity measurements described here, however, were carried out separately as part of a project linking spectral sensitivity to the protein sequences deduced from the opsin genes (Sharpe, Stockman, Jägle, Knau & Nathans, 1999a; Sharpe, Stockman, Jägle & Nathans, 1999b).

We are responsible for the analysis contained herein (aided by suggestions from the reviewers), but on some issues we have been guided by the committee's discussions and decisions. Two decisions that we have followed are: (1) that the cone fundamentals (at 2° and at other field sizes) should be defined in terms of the Stiles and Burch (1959) 10° CMFs; and (ii) that the luminosity function should be defined as a linear combination of the L- and M-cone spectral sensitivities, ignoring any small input from the S-cones.

We concur with both these decisions. First, as noted above, the Stiles and Burch (1959) 10° CMFs are the most secure and extensive of the available color match-

Table 1
Summary of sources and data concerning the fraction of male Caucasian subjects with the L(S180) polymorphism[a]

Source	Subjects	Fraction who are L(S180)
Winderickx et al. (1993)	109 (74 normals, 13 single-gene deuteranopes, 22 deutan defect)	0.560
Neitz and Neitz (1998)	130 (normals)	0.515
Sharpe et al. (1998a)	27 (single-gene deuteranopes)	0.741
Schmidt et al. (personal communication)	38 (36 normals, 2 single-gene deuteranopes)	0.605
Combined	304	0.563

[a] The mean fraction of 0.56 L(S180) to 0.44 L(A180) is the one used in the analysis.

ing data. Second, any small S-cone input to luminance is too strongly temporal-frequency- and adaptation-dependent to be usefully and simply defined as a fixed contribution to $V(\lambda)$ [the S-cone signal can, for example, subtract from flicker photometric sensitivity at low temporal frequencies, yet add to it at higher ones (Stockman et al., 1991)].

1.5. Molecular genetics

More information on this topic can be found elsewhere (e.g. Nathans, Merbs, Sung, Weitz & Wang, 1992; Sharpe et al., 1999b; Stockman, Sharpe, Merbs & Nathans, 2000). Here, we provide a brief summary of those areas that are relevant to this work.

The M- and L-cone photopigment genes lie in a head to tail tandem array on the q-arm of the X-chromosome. Each gene consists of six coding regions, called exons, which are transcribed to produce the opsin. Because the M- and L-cone photopigment genes are highly homologous and adjacent to one another, intragenic recombination between them is common and can lead to the production of hybrid or fusion genes, some of which code for anomalous pigments. Each hybrid gene can be identified by the site, usually between exons, at which the fusion occurs. For example, L3M4 indicates a hybrid gene in which exons 1–3 derive from an L-cone pigment gene and exons 4–6 from an M-cone pigment gene. Because exons 1 and 6 in the L- and M-cone pigment genes are identical, an L1M2 hybrid pigment gene encodes a de facto M-cone photopigment.

The classification of hybrid genes, and genes in general, is complicated by polymorphisms in the normal population, the most common of which is the frequent substitution of alanine by serine at codon 180 in exon 3. Of 304 genotyped Caucasian males, we estimate that 56% have the serine variant [identified as L(S180)] and 44% the alanine variant [identified as L(A180)] for their L-cone gene (see Table 1, which summarizes data from Winderickx, Battisti, Hibiya, Motulsky & Deeb, 1993; Neitz & Neitz, 1998; Sharpe et al., 1998a; Schmidt, Sharpe, Knau & Wissinger, personal communication).

The L-cone polymorphism, and its distribution in the normal population, must be considered when estimating the 'normal' L-cone spectral sensitivities. In contrast, the M(A180) versus M(S180) polymorphism for the M-cone pigment is much less frequent: 94% (Winderickx et al., 1993) or 93% (Neitz & Neitz, 1998) of males have the M(A180) variant. The nine protanopes in our study all have alanine at position 180 (Sharpe et al., 1998a), so that we have no examples of an M(S180) spectral sensitivity. Since the combination of an M(S180) spectral sensitivity with the mean M(A180) spectral sensitivity, weighted according to the ratio 6.5:93.5, would cause a λ_{max} change of about 0.17 nm (Sharpe et al., 1998a), we can reasonably ignore the effects of this polymorphism.

The spectral sensitivity of the photopigment that is encoded by the L2M3(A180) hybrid gene is practically indistinguishable from the photopigment encoded by the normal M(A180) [or L1M2(A180)] cone pigment gene, its λ_{max} being only 0.2 nm (Merbs & Nathans, 1992) or 0.0 nm (Asenjo, Rim & Oprian, 1994) or insignificantly (Sharpe et al., 1998a) different from that of the M(A180) cone pigment. Thus, spectral sensitivities from protanopes carrying either L1M2(A180) or L2M3(A180) genes in their opsin gene array can be reasonably combined to estimate the normal M-cone spectral sensitivities.

Dichromats with single photopigment genes in the M- and L-cone pigment gene array [e.g. L(A180), L(S180), L1M2(A180) or L2M3(A180)] are especially useful for measuring normal-cone spectral sensitivities, since they should possess only a single longer wavelength photopigment. Dichromats with multiple photopigment genes are less useful, unless the multiple genes produce photopigments with the same or nearly the same spectral sensitivities: for example, L1M2(A180) + M(A180) or L2M3(A180) + M(A180).

2. Methods

2.1. Subjects

The dichromats used in this study were part of a larger group of dichromats investigated by Sharpe et al. (1998a). For the Sharpe et al. study, 94 dichromat males were recruited in Freiburg, Tübingen and Vienna. Each subject was required to match the appearance of a standard monochromatic yellow light with various mixtures of monochromatic red and green lights, the so-called Rayleigh or traditional anomaloscope test

(Rayleigh, 1881). To qualify for the main study, the subjects had to be monochromats in the red–green range: that is, they needed to be able to produce a match by merely adjusting the intensity of the yellow light, regardless of the ratio of red to green in the mixture. Such behavior is consistent with the activity of a single longer wavelength photoreceptor (or multiple longer wavelength photoreceptors with spectral sensitivities too similar to influence the Rayleigh match). Of the dichromats who qualified, 29 were used in this study: for the measurement of M-cone spectral sensitivity, nine protanopes (six single-gene and three multiple-gene; mean age 31, range 18–45 years); and for the measurement of L-cone spectral sensitivity, 20 deuteranopes (all single-gene; mean age 29; range 20–43 years). Each subject was genotyped. For full details, see Sharpe et al. (1998a). Of the 20 deuteranopes, 15 were L(S180) and five were L(A180). Of the nine protanopes, three were L1M2(A180), three were L2M3(A180), one was L1M2(A180) + M(A180), and two were L2M3(A180) + M(A180).

The 22 color normals used in the luminosity measurements were all normal trichromats as defined by standard color vision tests, including the Rayleigh equation on the Nagel Type I anomaloscope. Each subject was also genotyped. Full details of the analysis will appear in a forthcoming publication (Schmidt, Sharpe, Knau & Wissinger, in preparation). Briefly, genomic DNA was obtained from the peripheral venous blood of each subject. To determine the number of L and M-cone opsin genes per X-chromosome, the genomic DNA was digested with the restriction enzyme Not *I*. The resulting DNA fragments were resolved using pulsed field gel electrophoresis. The Not *I* fragment containing the L- and M-pigment genes were then visualized by Southern blot hybridization with a human M-pigment cDNA probe (the methods are described in Macke & Nathans, 1997; Wolf, Sharpe, Schmidt, Knau, Weitz, Kioschis et al., 1999). In sizing the Not *I* segment, a repeat unit size of 40 kb and a single copy flanking sequence of 45 kb was calculated, based on a lambda-concatemer size standard. With the use of primers in the flanking intron regions, exons 2–3 of the L-cone opsin gene in each sample were amplified by PCR. One primer was specific for the extra insert in exon 1 in the L-cone opsin gene; the other for the 3′ end of exon 3. The PCR products were purified and both strands sequenced with a ABI 377 Sequencer (see Sharpe et al., 1998a). Other sources (Sharpe et al., 1999b) explain these procedures in more detail. For this work, we were principally concerned with whether each subject's normal L-cone gene was L(S180) or L(A180). The number of M-cone genes possessed by each subject, which varies from 1 to 5, does not correlate with changes in luminous efficiency (Knau, Schmidt, Wolf, Wissinger & Sharpe, 1999). Of the 22 subjects, 13 were L(S180) and nine were L(A180).

2.2. Apparatus

Measurements were made on a conventional Maxwellian-view optical system illuminated by a 75-W xenon arc lamp (Osram) run at constant current. The images of the xenon arc at the plane of the observer's pupil were less than 1.5 mm in diameter. Two channels provided the alternating 2° diameter test and reference fields, and a third the 18° diameter steady background field. Mechanical shutters driven by a computer-controlled square-wave generator were positioned in each channel near focal points of the xenon arc. The optical waveforms so produced were monitored periodically using a Pin-10 diode (United Detector Technology) and oscilloscope.

Fine control over the luminance of the stimuli was achieved by variable, 2 log unit (Spindler & Hoyer) or 4 log unit (Rolyn Optics) neutral density wedges positioned at xenon arc image points, and by fixed neutral density filters inserted in collimated portions of the beams. The position of the observer's head was maintained by a rigidly mounted dental wax impression.

The wavelengths of the alternating test and reference fields were selected by grating monochromators (Jobin-Yvon H-10 Vis) with 0.5 mm entrance and exit slits. Their spectral outputs were triangular functions of wavelength with bandwidths at half maximum output (the 'full width at half maximum' or FWHM) of approximately 4 nm. The wavelength of the reference light was always set to 560 nm, while that of the test light was varied from 400 to 700 nm in 5 nm steps (although protanopes typically ran out of enough light to set a flicker null at 680 nm). At wavelengths longer than 560 nm, a glass cut-off filter (Schott OG550) was inserted to attenuate the shorter wavelength portion (< 530 nm) of a small skirt of scattered light leaked by the monochromator (which anyhow was too small to be visually significant in these experiments). The wavelength of the 18° diameter background field was selected by a third grating monochromator (Jobin-Yvon H-10 Vis) with 2 mm entrance and exit slits. Its output was also a triangular function of wavelength, but with an FWHM of 17 nm. Infra-red radiation was eliminated by heat absorbing glass (Schott) placed early in each beam.

2.3. Calibration

The radiant fluxes of test and background fields were measured in situ at the plane of the observers' pupil. Extensive calibrations were conducted at both sites where the spectral sensitivities were measured: Freiburg and Tübingen. In Freiburg, the radiant fluxes were measured with a radiometer (United Detector Technology, Model S370 Optometer); in Tübingen, with a calibrated silicon photodiode (Model SS0-PD50-6-BNC, Gigahertz-Optics) and a picoammeter (Model

486, Keithley). We carried out our own additional calibration checks. Both instruments were cross-calibrated against: (i) another silicon photodetector (Gigahertz-Optics), which was calibrated against the German National Standard (Braunsweig), and (ii) a recently calibrated radiometer (Graseby, Model S370 Optometer) transported from San Diego, the calibration of which was traceable to the US National Standard. The devices agreed to within 0.01 $\log_{10}$ unit from 400 to 700 nm.

The monochromators and interference filters were also calibrated in situ. In Freiburg, the spectral calibrations were carried out with a Photo Research, PR-704 spectroradiometer (Spectra-Scan), and in Tübingen with an Instrument Systems CAS-140 Spectroradiometer (Instrument Systems GmbH, Compact Array Spectrometer). The resolution of the Freiburg and Tübingen instruments were better than 0.5 and 0.2 nm, respectively. The wavelength scales of the two spectroradiometers and the Jobin-Yvon monochromators were calibrated against a low pressure mercury source (Model 6035, L.O.T.-Oriel GmbH).

2.4. Procedures

2.4.1. Cone spectral sensitivities

Corneal spectral sensitivities were measured by heterochromatic flicker photometry (HFP) in dichromats. The 2° reference light (560 nm) was alternated at 25 Hz, or in preliminary measurements, at 16 Hz, in opposite phase with a superimposed test light, the wavelength of which was varied in 5-nm steps over the spectrum from 400 to 700 nm. For some subjects, the shorter and longer wavelength regions were measured during separate runs.

The two targets were presented on a 430-nm background field of 11.00 log quanta $\sec^{-1}$ $\deg^{-2}$ (3.08 log photopic td or 4.71 log scotopic td), which saturated the rods and prevented the S cones from contributing to the measurements. S-cone-mediated detection was further disadvantaged by the flicker frequency (which was always 25 Hz at short wavelengths) and the HFP task (Eisner & MacLeod, 1980; Stockman et al., 1991).

At the start of the spectral sensitivity experiment, the subject was asked to adjust the intensity of the 560-nm flickering reference light until the flicker appeared to be just at threshold. After five settings had been made, the mean threshold setting was calculated and the reference light was set 0.2 $\log_{10}$ unit above this value. The test light was then added to the reference light in counterphase. The subject was asked to adjust the intensity of the flickering test light until the flicker percept disappeared or was minimized. This procedure was repeated five times at each of up to 31 wavelengths. After each setting, the intensity of the flickering test light was randomly reset to a higher or lower intensity, so that the subject had to readjust the intensity to find the best setting. The target wavelength was randomly varied. From two to six complete runs were carried out by each subject. Thus, each data point represents between ten and 30 threshold settings.

Further details about the procedure and data collection, as well as the analysis of the individual spectral sensitivity data and λ_{max} estimates can be found in Sharpe et al. (1998a).

2.4.2. Luminous efficacy

The luminous efficacy measurements will be described in more detail in a forthcoming paper by Sharpe, Jägle, Serey, Knau & Stockman (in preparation). They were measured using the same apparatus and procedure used for the cone spectral sensitivity measurements, except that the two 2° diameter flicker photometric targets were presented on a 16° diameter xenon arc white (6500 K) background of 3.00 log ph td (i.e. sufficiently luminous to saturate the rod response). Again, the reference target of 560 nm was set to 0.2 log unit above flicker threshold. The flicker frequency was 25 Hz. From three to six runs were carried out by each subject. Significantly, the identity of the amino acid at codon 180 had been identified in each of the subjects who performed these experiments, so that we could identify their L-cone phenotype. As described below, the mean luminous efficiency function was averaged by weighting the L(S180) and L(A180) means according to the ratio of L(S180) to L(A180) found in the male Caucasian population (i.e. 0.56 L(S180) to 0.44 L(A180), see Table 1).

2.5. Curve fitting

All curve fitting was carried out with the standard Marquardt–Levenberg algorithm implemented in SigmaPlot (SPSS Inc, Chicago), which was used to find the coefficients (parameters) of the independent variable or variables that gave the 'best fit' between our various models and the data. This algorithm seeks the values of the parameters that minimize the sum of the squared differences between the values of the observed and predicted values of the dependent variable or variables. Fits were made to log spectral sensitivity data.

3. Results

3.1. Spectral sensitivity data

Fig. 1 shows the mean data obtained by Sharpe et al. (1998a) from 15 L(S180) single-gene deuteranopes (black circles), from five L(A180) single-gene deuteranopes (gray circles), and from nine protanopes (gray diamonds). The individual spectral sensitivity data for

each subject can be found in Figs. 1–5 of Sharpe et al. (1999a). The spectral sensitivity functions for the L(S180) and L(A180) groups are separated in λ_{max} by ~ 2.7 nm (Sharpe et al., 1998a). As noted above, of the nine protanopes, three had a single L1M2(A180) gene, three had a single L2M3(A180) gene, one had an L1M2(A180) and an M(A180) gene, and two had an L2M3(A180) and an M(A180) gene.

Factors other than gene type, such as macular and photopigment optical densities, can also affect corneally-measured spectral sensitivities. Thus, it is important to compare the spectral sensitivities of our dichromats with those of color normals to ensure that the dichromat data are not somehow atypical. We therefore compared the dichromat data with the mean M-cone (white dotted triangles) and L-cone (white dotted inverted triangles) data of Stockman et al. (1993a). The Stockman, MacLeod and Johnson data, which are from normals mainly and some dichromats, agree well with the protanope and deuteranope data. As expected, since the Stockman, MacLeod and Johnson subjects should include examples of both variants of the L-cone photopigment, their mean L-cone data lie between the L(S180) and L(A180) means.

We next consider the relationship of the mean cone spectral sensitivities to color matching data. In general, it is preferable to define the cone fundamentals in terms of color matching data, rather than in terms of directly measured spectral sensitivity data, since the former tend to be more precise and noise-free. Thus, the spectral sensitivity data are used here primarily to guide the choice of linear transformation from the color matching functions to the cone fundamentals.

3.2. Derivation of M- and L-cone fundamentals

The definition of the M- and L-cone spectral sensitivities in terms of $\bar{r}(\lambda)$, $\bar{g}(\lambda)$ and $\bar{b}(\lambda)$ requires knowledge of four unknowns (see Eq. (3), above), $\bar{m}_R/\bar{m}_B$, $\bar{m}_G/\bar{m}_B$, $\bar{l}_R/\bar{l}_B$ and $\bar{l}_G/\bar{l}_B$, thus:

$$\frac{\bar{m}_R}{\bar{m}_B}\bar{r}(\lambda)+\frac{\bar{m}_G}{\bar{m}_B}\bar{g}(\lambda)+\bar{b}(\lambda)=k_m\bar{m}(\lambda) \quad (4)$$

and

$$\frac{\bar{l}_R}{\bar{l}_B}\bar{r}(\lambda)+\frac{\bar{l}_G}{\bar{l}_B}\bar{g}(\lambda)+\bar{b}(\lambda)=k_l\bar{l}(\lambda) \quad (5)$$

We used the new red–green dichromat data to estimate the unknowns in Eqs. (4) and (5). Our strategy, which was similar to that of Stockman et al. (1993a), was first to find the linear combinations of the Stiles and Burch (1955) 2° CMFs that best fit the mean 2° spectral sensitivity data for, in our case: (i) L1M2(A180)/L2M3(A180) protanopes; (ii) L(S180) deuteranopes; and (iii) L(A180) deuteranopes, so producing Stiles and Burch (1955) 2° CMF based estimates of the cone spectral sensitivities that are representative of polymorphic variation in the normal population. In the fitting procedure, we allowed for differences in macular and lens pigment densities between the mean observers represented by our data and the mean observer represented by the Stiles and Burch 2° CMFs. The lens and macular pigment differences given below are best fitting differences that were determined simultaneously with the best fitting linear combination of the CMFs. As previously noted, all fits minimized the squared differences between the log spectral sensitivities.

Our working hypothesis in making these fits is that the cone spectral sensitivities should be a linear combination of the CMFs (see Eqs. (2)–(5)) — after appropriate (and necessary) adjustments in macular, and lens density (and, from 2 to 10°, adjustments in photopigment optical density). To a first approximation, this working hypothesis is clearly supported by the curve fits (see Figs. 3–6). The residuals that remain are likely to be due to other known sources of individual differences, such as differences in photopigment optical density and λ_{max}, instrumental and experimental differences, experimental noise, and other unknown factors. Reassuringly, despite all these potential sources of error, the residuals are invariably small (see lower panels of Figs. 3–6). Curve fitting, however, has several dangers, not least of which is that the fits may obscure real, underlying differences between the sets of data. Until CMFs and cone spectral sensitivities are measured in the same observers, however, or are accompanied by careful measurements of the factors that cause individual differences, such uncertainties will persist.

The macular and lens pigment density spectra used in the fits are those tabulated in Table 2 of Appendix A. Their derivation is explained next.

3.2.1. Macular pigment

Fig. 2a shows estimates of the macular pigment density spectrum by Vos (1972) (white circles) and by Wyszecki and Stiles (1982) (black circles), both of which are the 'weighted' means of data from several sources, including sensitivity measures that confound changes in macular pigment density with eccentricity with changes in photopigment optical density (see Sharpe, Stockman, Knau & Jägle, 1998b). The MSP estimate by Snodderly, Brown, Delori and Auran (1984) is also shown. The macular pigment density spectrum that we have adopted is indicated by the continuous line, and is tabulated in Table 2. It is based on a spectrophotometer output provided by Bone (personal communication), which also appears at wavelengths longer than 420 nm in Fig. 3 of Bone, Landrum and Cains (1992). The spectrum is that of lutein and zeaxanthin mixed in the same ratio as found in the foveal region and incorporated into phospholipid membranes (see Bone et al., 1992 for further details).

Stockman et al. (1999) first adopted the proposed macular pigment density spectrum in their analysis of individual S-cone spectral sensitivity data, since they found that, in contrast to the other spectra shown in Fig. 2a, it produced plausible estimates of the S-cone photopigment optical density change from central to peripheral retina. As can be seen in Fig. 2a, the differences between the spectra are mainly at very short wavelengths, where the reliability of the Vos and of the Wyszecki and Stiles spectra is questionable, and the MSP data non-existent. Above 420 nm, the proposed spectrum differs from that of Vos by less than 0.02.

3.2.2. Lens pigment

Fig. 2b shows estimates of the lens pigment density spectrum by Wyszecki and Stiles (1982) (black circles) and van Norren and Vos (1974) (white circles). The proposed lens pigment spectrum (continuous line) is a slightly modified version of the van Norren and Vos (1974) spectrum. The modifications were made by Stockman et al. (1999) to remove a small discontinuity in the S-cone photopigment optical density spectrum calculated from the S-cone fundamental (see their Fig. 14). As can be seen in Fig. 2b, the modifications are small, and are almost certainly less than the error inherent in the van Norren and Vos lens density estimate.

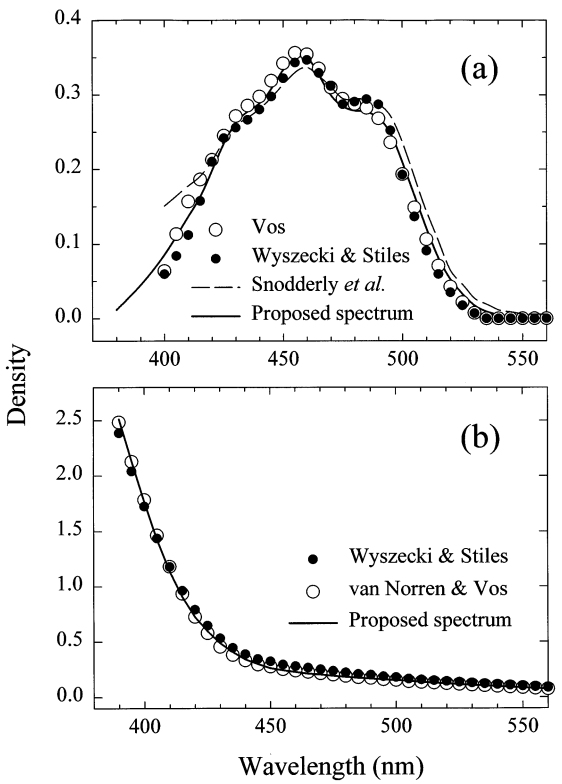

Fig. 2. (a) Estimates of the macular pigment optical density spectra by Wyszecki and Stiles (1982) (black circles), Vos (1972) (open circles), and Snodderly et al. (1984) (dashed lines) compared with the macular pigment spectrum tabulated in Table 2 (continuous line), which is based on measurements by Bone (personal communication). (b) Estimates of the lens optical density spectra by Wyszecki and Stiles (1982) (black circles) and van Norren and Vos (1974) (white circles) compared with the lens spectrum tabulated in Table 2, which is a modified version of the van Norren and Vos function. The lens spectra have been adjusted in overall density to align with the proposed function.

3.3. Stiles and Burch (1955) 2° based fundamentals

The linear combination of the Stiles and Burch (1955) 2° CMFs that best fits the mean L1M2(A180)/L2M3(A180) protanope data (gray diamonds) with best fitting macular and lens pigment density adjustments is shown as the continuous line in Fig. 3a. The best fitting values (ignoring the vertical scaling constant required to align the function with the data) are $\bar{m}_R/\bar{m}_B = 0.29089$ and $\bar{m}_G/\bar{m}_B = 12.24415$. The best fitting density adjustments suggest that, compared with the mean densities of the Stiles and Burch (1955) observer, the L1M2(A180)/L2M3(A180) observers' average macular pigment is lower by 0.03 in peak density (at 460 nm), and their average lens pigment is higher in density by 0.09 at 400 nm. Fig. 3b shows the residuals (gray diamonds). The fit to the data is good throughout the spectrum with an rms (root-mean-squared) error of 0.021 log unit. Also shown are the mean Stockman et al. (1993a) M-cone experimental data (white dotted triangles) aligned with the Stiles & Burch 2° cone fundamental at middle- and long wavelengths, where both data sets agree well. The agreement at middle and long-wavelengths suggest that the normals and protanopes have comparable photopigment optical densities.

Fig. 4a shows the linear combination of the Stiles and Burch (1955) 2° CMFs that best fits the mean L(S180) deuteranope data (black circles) with macular and lens pigment density adjustments. The best fitting values are $\bar{l}_R/\bar{l}_B = 5.28554$ and $\bar{l}_G/\bar{l}_B = 16.80098$. The best fitting density adjustments indicate that, compared with the mean densities of the Stiles and Burch (1955) observer, the L(S180) observers' average macular pigment is higher by 0.08 in peak density, and their average lens pigment is lower in density by 0.07 at 400 nm. Again the fit to the data is good throughout the spectrum with an rms error of 0.018 log unit. Also shown are the mean Stockman et al. (1993a) L-cone data (white dotted inverted triangles). In contrast to the M-cone data, the Stockman, MacLeod and Johnson data tend to fall more steeply than the L(S180) data at longer wavelengths.

Fig. 5a shows the linear combination of the Stiles and Burch (1955) 2° CMFs that best fits the mean L(A180) deuteranope data (gray circles) with macular and lens pigment density adjustments. The best fitting values are $\bar{l}_R/\bar{l}_B = 4.15278$ and $\bar{l}_G/\bar{l}_B = 16.75822$. Only

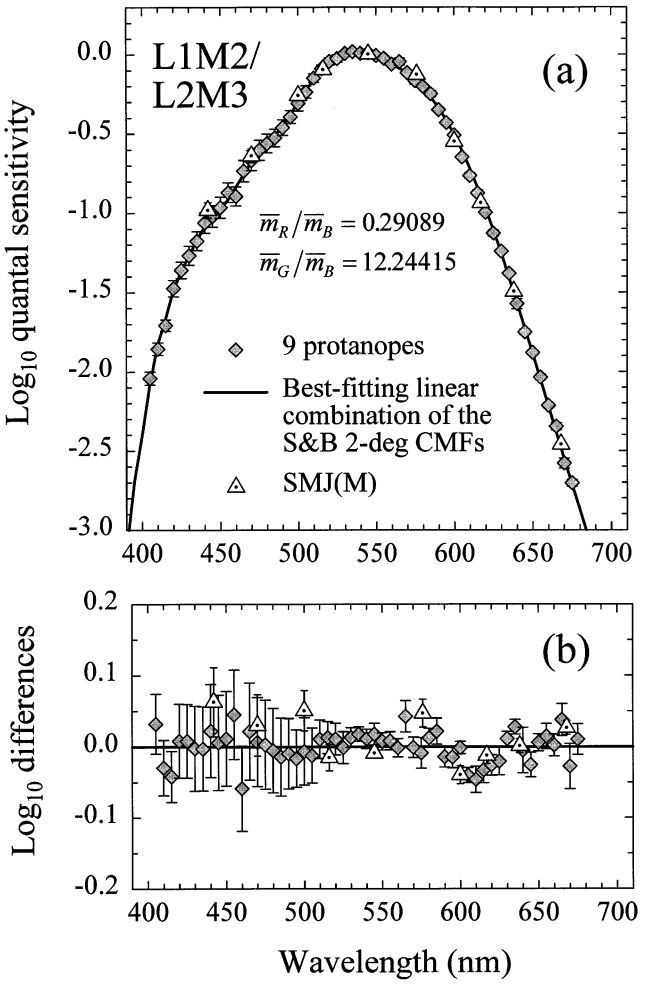

Fig. 3. Fits of the 2° CMFs to the protanope data. (a) Mean L1M2(A180) and L2M3(A180) protanope data (gray diamonds) from Sharpe et al. (1998a), mean M-cone data (white dotted triangles) from Stockman et al. (1993a) and the linear combination of the Stiles and Burch (1955) CMFs (continuous line) that best fits the mean protanope data. The protanope data have been adjusted in lens and macular pigment density to best fit the CMFs. The mean Stockman, MacLeod and Johnson M-cone data are unadjusted. (b) Differences between the protanope data and the linear combination of the CMFs (gray diamonds), and between the mean M-cone data and the CMFs (white dotted triangles). Error bars are ± 1 standard error of the mean. For further details see text.

two out of the five L(A180) subjects made measurements over the whole spectral range, the remaining three making measurements from only 470 nm to long wavelengths. Although the mean data for the whole group are shown (gray circles), the fit of the CMFs was carried out simultaneously to the mean data for two groups separately by assuming that they had the same $\overline{l}_R/\overline{l}_B$ and $\overline{l}_G/\overline{l}_B$ values but different lens and macular pigment densities (and scaling constants) (the fit cannot be made directly to the overall mean shown in Fig. 5, because the mean lens and macular densities are different below 470 nm (where $n = 2$) and above it (where $n = 5$)). The best fitting density adjustments (averaged across all five subjects) suggest that, compared with the mean Stiles and Burch (1955) observer, the L(A180) observers' average macular pigment is higher by 0.11 in peak density, and their average lens pigment is lower in density by 0.18 at 400 nm. Since the mean data are averaged from relatively small numbers of subjects the scatter around the fit is larger, with an rms error of 0.040 log unit, but the fit is good. The mean Stockman et al. data (1993a) L-cone data are shown again (white dotted inverted triangles). In contrast to the L(S180) case, the Stockman, MacLeod and Johnson data tend to fall less steeply than the dichromat data at longer wavelengths.

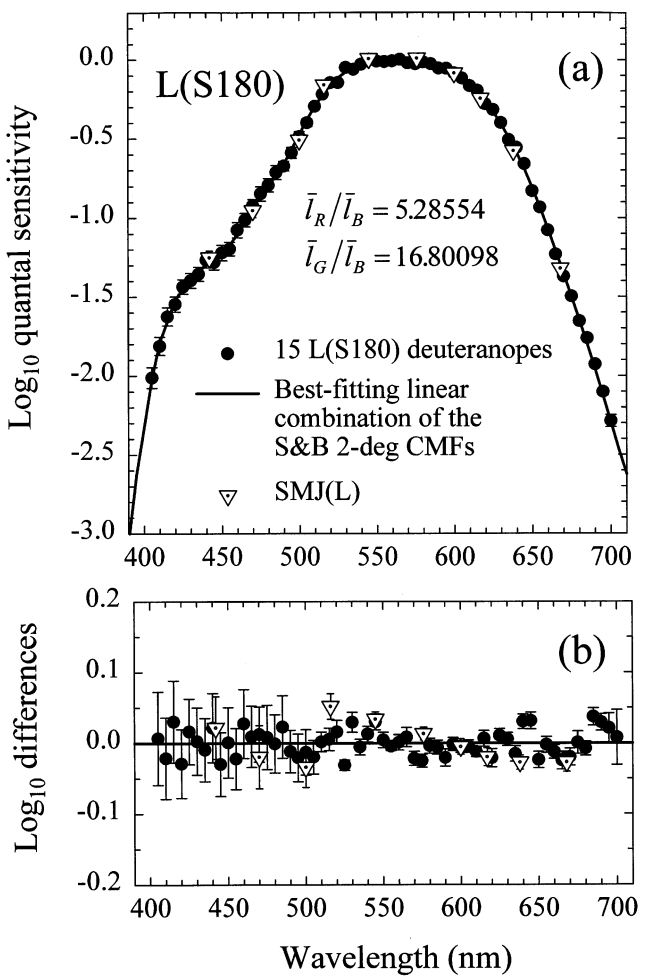

Fig. 4. Fits of the 2° CMFs to the L(S180) data. (a) Mean L(S180) deuteranope data (black circles) from Sharpe et al. (1998a), mean L-cone data (white dotted inverted triangles) from Stockman et al. (1993a) and the linear combination of the Stiles and Burch (1955) CMFs (continuous line) that best fits the mean L(S180) data. The L(S180) data have been adjusted in lens and macular pigment density to best fit the CMFs. The mean Stockman, MacLeod and Johnson L-cone data are unadjusted. (b) Differences between the L(S180) data and the linear combination of the CMFs (black circles), and between the mean L-cone data and the CMFs (white dotted inverted triangles). Error bars are ± 1 standard error of the mean. For further details see text.

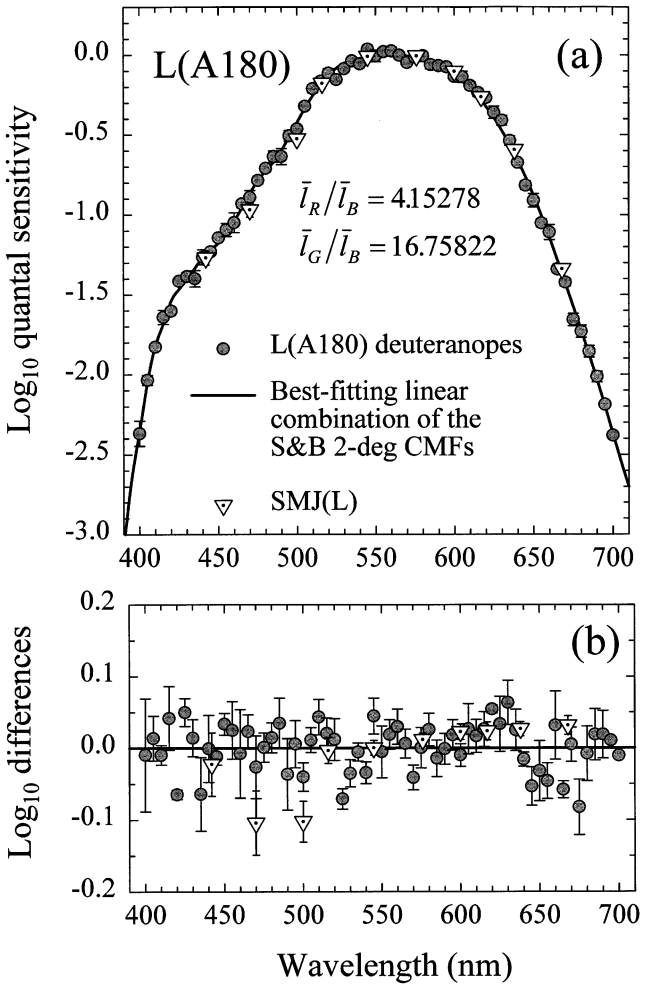

Fig. 5. Fits of the 2° CMFs to the L(A180) data. (a) Mean L(A180) data for all five deuteranopes from 470 to 700 nm, and for the two deuteranopes who made short-wavelength measurements from 400 to 465 nm (gray circles) from Sharpe et al. (1998a), mean L-cone data (white dotted inverted triangles) from Stockman et al. (1993a) and the linear combination of the Stiles and Burch (1955) CMFs (continuous line) that best fits the L(A180) data. The L(A180) data have been individually adjusted in lens and macular pigment density to best fit the CMFs. The Stockman, MacLeod and Johnson mean L-cone data are unadjusted. (b) Differences between the L(A180) data and the linear combination of the CMFs (gray circles), and between the mean L-cone data and the CMFs (white dotted inverted triangles). Error bars are ± 1 standard error of the mean. For further details see text.

The long-wavelength differences between the normal L-cone data of Stockman et al. (1993a) and the L(S180) and L(A180) data are expected. In contrast to the single-gene L(S180) and L(A180) dichromats, the subjects used by Stockman, MacLeod and Johnson would have a mixture of L(S180) and L(A180) photopigment genes. Consequently, the L-cone spectral sensitivity function obtained by Stockman et al. (1993a) *should* be intermediate in spectral position between the mean L(S180) and L(A180) functions — as is found.

To obtain an estimate of the mean L-cone fundamental, we weighted the L(A180) and L(S180) $\bar{l}_G/\bar{l}_B$and $\bar{l}_R/\bar{l}_B$ values according to the ratio of 0.56 L(S180) to 0.44 L(A180) found in the normal, male Caucasian population (see Table 1), and averaged them together. Thus, the mean 2° L-cone fundamental based on the Stiles and Burch 2° CMFs is defined by $\bar{l}_G/\bar{l}_B = 16.782165$ and $\bar{l}_R/\bar{l}_B = 4.787127$.

3.4. Stiles and Burch (1959) 10° based fundamentals adjusted to 2°

Having derived M- and L-cone fundamentals using the 2° CMFs of Stiles and Burch (1955), we next defined the M- and L-cone spectral sensitivities in terms of the Stiles and Burch (1959) 10° CMFs corrected to 2°. One reason for preferring fundamentals based on the 10° CMFs is that they produce cone fundamentals that are less noisy, especially at shorter wavelengths, than the 2° CMFs (see Figs. 12–15 of Stockman et al., 1993a). Another is that the 10° CMFs are based on 49 observers, instead of the ten used in the 2° study, so that they are more likely to represent the mean color matches of the normal population.

Unfortunately, direct fits of the 10° CMFs to the dichromat data proved to be impracticable, mainly because the differences between the L-cone phenotypes tended to be accounted for by inappropriate changes in photopigment optical density rather than appropriate changes in the CMF weights. Consequently, following the method of Stockman et al. (1993a), we used the 2° cone fundamentals defined previously as an intermediate step in the derivation of the 10° based fundamentals. With this step, the fit of the 10° CMFs to the 2° functions was better constrained, and produced plausible density changes. A secondary advantage of this method is that it provides a tangible and definable link between the 2 and 10° CMFs of Stiles and Burch.

We derived the 10° based cone fundamentals by a curve fitting procedure in which we found the linear combinations of the Stiles and Burch (1959) 10° CMFs that best fit the Stiles and Burch (1955) 2° M- and L-cone fundamentals, including optimized adjustments in macular, lens and photopigment densities. The adjustments from the 10° CMFs to the 2° fundamentals were: (i) for macular pigment density, a change from a peak of 0.095 to a peak of 0.35; (ii) for peak photopigment optical density, a change from 0.38 to 0.50; and (iii) for lens pigment density, a change from a density of 1.76 at 400 nm to 1.63 at 400 nm. The fits were restricted to 395–725 nm in order to keep them within the range of measured color matches (which is 392.2–727.3 nm for the Stiles and Burch 2° measurements). The resulting best fitting linear combinations were, for M, $\bar{m}_R/\bar{m}_B = 0.168926$ and $\bar{m}_G/\bar{m}_B = 8.2846201$, and, for L, $\bar{l}_R/\bar{l}_B = 2.846201$ and $\bar{l}_G/\bar{l}_B = 11.092490$. The *rms* error for the fits, which were carried out simultaneously, was only 0.012 log unit for both fundamentals. The 2

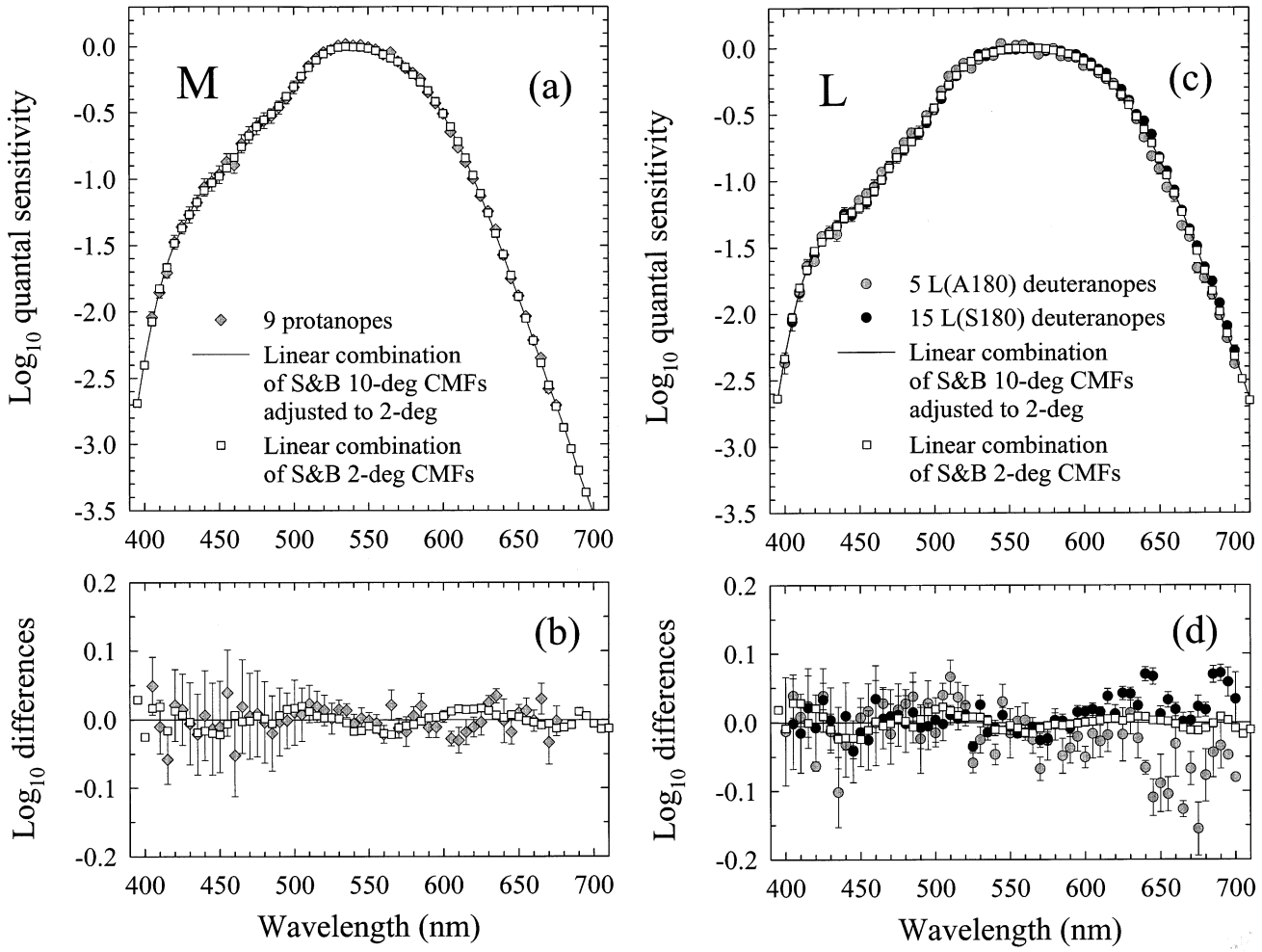

Fig. 6. (a) Linear combination of the Stiles and Burch (1959) 10° CMFs adjusted to 2° (continuous line) that best fits the Stiles and Burch (1955) based 2° M-cone fundamental (open squares), and the macular- and lens-adjusted 2° protanope data (gray diamonds) from Fig. 3. The best fitting linear combination is $\bar{m}_R/\bar{m}_B = 0.168926$ and $\bar{m}_G/\bar{m}_B = 8.265895$. (b) Residuals from (a). (c) Linear combination of the Stiles and Burch (1959) 10° CMFs adjusted to 2° (continuous line) that best fits the Stiles and Burch (1955) based 2° L-cone fundamental (open squares), and macular- and lens-adjusted L(S180) (dark circles) and L(A180) (gray circles) deuteranope data. The best fitting linear combination is $\bar{l}_R/\bar{l}_B = 2.846201$ and $\bar{l}_G/\bar{l}_B = 11.092490$. (d) Residuals from (c).

and 10° cone fundamentals based on this transformation are given in Table 2.

Prior to the fitting procedure, we had to choose the absolute values of (i) the peak macular pigment density; (ii) the photopigment optical density; and (iii) the lens pigment density. These choices are reviewed and discussed in more detail elsewhere (Stockman et al., 1993a; Stockman & Sharpe, 1999). In summary, the peak macular pigment density of 0.35 was averaged from the 2° macular pigment density estimates by Smith and Pokorny (1975), Stockman et al. (1993a), Stockman et al. (1999); and Sharpe et al. (1998a) (see also Vos, 1972). The choice of 0.5 for the photopigment optical density for a 2° target was based on a review of the available estimates (see Stockman & Sharpe, 1999), but given the range of estimates must be considered approximate. Fortunately, within limits, the choice of the peak photopigment optical density has little influence on the best fitting linear combination. The best fitting lens pigment density difference given above represents a difference in density between the groups of observers used to measure the CMFs, rather than a difference resulting from the change in target size from 2 to 10°. The choice of lens density for the 10° CMFs and for the proposed fundamentals, which is 1.7649 at 400 nm (see Table 2), was guided by several considerations, including the differences between the S-, M- and L-cone fundamentals derived from the Stiles and Burch 2 and 10° CMFs, an analysis of individual L- and M-cone spectral sensitivity spectral data (Sharpe et al., 1998a), and calculations of the photopigment optical density spectra from the cone fundamentals (see Fig. 12). Importantly, the assumed lens densities produce photopigment optical density spectra of approximately invariant shape when shifted along an abscissa of log wavelength (see Fig. 12b).

The Stiles and Burch (1955) based 2° M- and L-cone fundamentals (small white squares), and the best fitting

linear combinations of the Stiles and Burch (1959) 10° CMFs adjusted to 2° (continuous lines) are shown in Fig. 6a (M-cone) and Fig. 6c (L-cone). The corresponding residuals are shown in Fig. 6b (M-cone) and Fig. 6d (L-cone). Above 450 nm, the fits are excellent with residuals of less than ± 0.02 log unit. At wavelengths shorter than 450 nm, the agreement is slightly worse with residuals of up to ± 0.04 log unit. Such good agreement is perhaps not surprising, since the same apparatus was used for both the 2 and 10° CMF measurements, and the ten subjects who participated in the 2° study also participated in the 10° one.

We emphasize that the small residuals shown in Fig. 6b,d (open squares) are between the 2° cone fundamentals based on the Stiles and Burch (1955) 2° CMFs and the Stiles and Burch (1959) 10° CMFs. To allow comparisons with our original data, the 2° macular- and lens-adjusted protanope data (Fig. 6a,b: gray diamonds), L(S180) deuteranope data (Fig. 6c,d: dark circles), L(A180) deuteranope data (Fig. 6c,d: gray circles) are also shown. The L-cone comparison in Fig. 6c,d shows, as expected, that the L-cone fundamental is intermediate between the L(S180) and L(A180) deuteranope data at longer wavelengths. The M-cone comparison in Fig. 6a,b is more instructive, since the 10 and 2° CMF based fundamentals can be compared directly with the protanope data. As can be seen, both agree well. In terms of the rms of the residuals, the 10° based fundamentals agree with the protanope data (diamonds, Fig. 6b) marginally better than the 2° based fundamentals (diamonds, Fig. 3b).

3.5. Tritanopic color matches

Tritanopic matches provide a useful means of testing between existing M- and L-cone fundamentals. Since tritanopes lack functioning S-cones, their color matches should be predicted, within the limits imposed by individual differences in spectral sensitivity (such as those caused by the L(A180) versus L(S180) polymorphism), by any plausible estimates of the M- and L-cone spectral sensitivities.

In Figs. 7 and 8, we have replotted several 2° M- and L-cone cone fundamentals in the form of W.D. Wright (WDW) tritanopic $g(\lambda)$ coordinates by transforming them to Wright's primaries of 480 and 650 nm and then equating them at 582.5 nm (the WDW $r(\lambda)$ coordinates are simply 1-$g(\lambda)$). Two advantages of plotting the tritanopic predictions in this way are that WDW coordinates are independent of individual differences in lens and macular pigment densities, and that Wright's (1952) tritanope data are tabulated in the same form, so allowing straightforward comparisons. The tritanopic matches predicted by a $g(\lambda)$ function are any two wavelengths that have the same $g(\lambda)$ value.

Fig. 7 shows the $g(\lambda)$ function (diamonds, continuous line) predicted by the 2° M- and L-cone fundamentals from Table 2. Overall, the agreement with Wright's data (gray dotted circles) is fairly good, except at 410 nm and between 540 and 560 nm. Given, however, that Wright's data are for a 1.33° target, rather than the more standard 2° target used here, we carried out an independent check of tritanopic matches using a 2° target (Stockman & Sharpe, 2000).

Pokorny and Smith (1993) suggested that a simple means of testing between cone fundamentals is to determine the spectral lights that tritanopes confuse with the 404.7 and 435.8 nm Hg lines (which, when isolated, are nearly monochromatic). These should be predicted, at least approximately (see below), by any viable estimate of the M- and L-cone spectral sensitivities. Following up on their suggestion, Stockman and Sharpe (2000) carried out matching experiments separately in Tübingen and in San Diego under intense short-wavelength adapting conditions that induced artificial tritanopia in normals. The matches for five normals and one tritanope measured in Tübingen (open circles) and three normals and one tritanope measured in San Diego (open squares) are shown in Fig. 7.

The Hg lines at 404.7 and 435.8 nm are broadened and shifted to longer wavelengths in high-pressure Hg arc lamps (Elenbaas, 1951), so that the effective spectral 'lines' were 405.8 and 438.4 nm in Tübingen (where an interference filter was used that slightly skewed the spectral distribution) and 405.8 and 436.5 nm in San Diego. The mean matches were: 405.8 matches 556.9 nm; 436.5 matches 495.1 nm; and 438.4 matches 491.2 nm (see Stockman & Sharpe, 2000).

These matches can be compared with the predictions of the proposed 2° M- and L-cone fundamentals (filled diamonds, continuous line), which can be seen by following the outlines of the three large rectangles from 405.8, 436.5 and 438.4 nm. They are 556.1 nm for the 405.8 nm match (0.8 nm too short); 493.8 nm for the 436.5 nm match (1.3 nm too short); and 490.5 nm for the 438.4 nm match (0.7 nm too short).

To put these discrepancies into context, we estimated the variability in the matches that is likely to be caused by the common L(A180) versus L(S180) polymorphism (see, for details, Stockman & Sharpe, 2000). Fig. 8 shows the three $g(\lambda)$ functions predicted by L (continuous line, as Fig. 7), L(S180) (open inverted triangles) and L(A180) (open triangles). The change from L to L(A180) shifts the predicted 405.8, 436.5 and 438.4 nm matches by -0.5, -3.6 and -3.7 nm, respectively, while the change from L to L(S180) shifts them by $+0.4$, $+3.1$ and $+2.6$ nm, respectively, as noted in the figure. The L(S180) and L(A180) predictions delimit the range of matches that should be caused by the L-cone polymorphism, while the L (mean) predictions

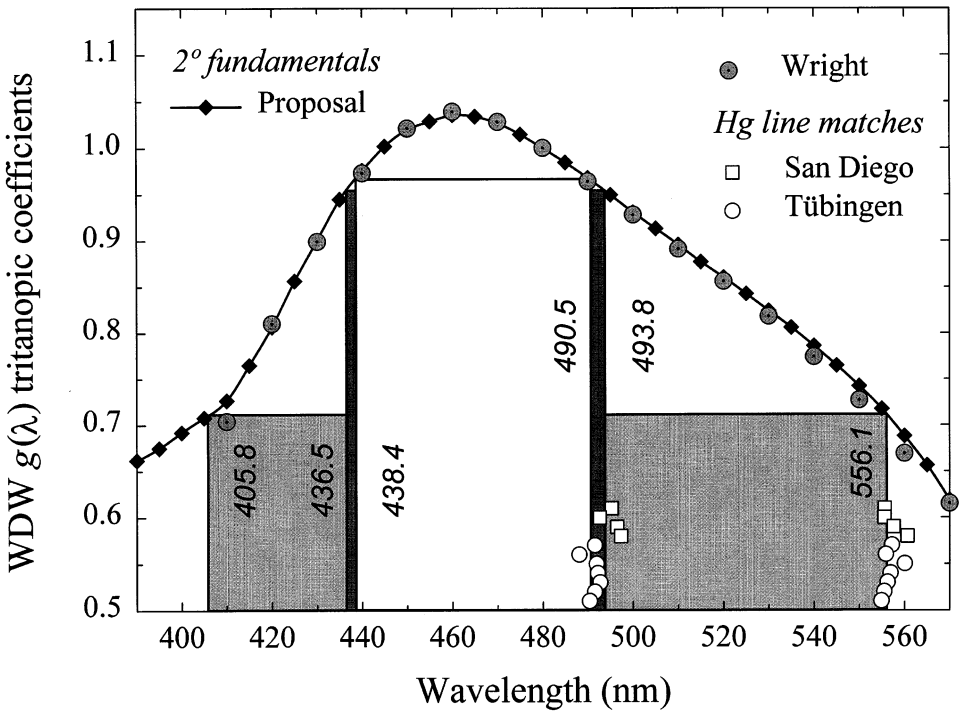

Fig. 7. Tritanopic color matches and M- and L-cone spectral sensitivities. Tritanopic $g(\lambda)$ predictions of the proposed 2° M- and L-cone fundamentals tabulated in Table 2 (filled diamonds, continuous line); and the wavelengths found by eleven subjects (nine color normals and two tritanopes) to match either a 405.8- or a 436.5-nm target light (open squares, San Diego) or a 405.8- or 438.4-nm target light (open circles, Tübingen) under conditions that produce tritanopia in the normals. The matches to the 405.8-, 436.5- and 438.4-nm lights predicted by the optimized fundamentals are 490.5, 493.8 and 556.1 nm, respectively, as indicated by the outlines of the three large gray or white rectangles. Also shown are Wright's tritanopic $g(\lambda)$ coefficients (gray dotted circles) (Wright, 1952).

indicate the likely mean. The predictions of our fundamentals lie within the range of matches expected from differences between the L(A180) and L(S180) spectral sensitivities.

For comparison, Fig. 8 also shows the $g(\lambda)$ predicted by the Stockman et al. (1993a) (longer dashed line) and Smith and Pokorny (1975) (dot-dashed line) fundamentals. The former predicts a match 561.2 nm for the 405.8 nm match (4.3 nm too long); 493.0 nm for the 436.5 nm match (2.1 nm too short); and 489.7 nm for the 438.4 nm match (1.5 nm too short), whereas the latter predict 544.4 nm for the 405.8 nm match (12.5 nm too short); 500.4 nm for the 436.5 nm match (5.3 nm too long); and 496.9 nm for the 438.4 nm match (5.7 nm too long). All these predictions, except the 436.5 and 438.4 nm match predictions of Stockman, MacLeod and Johnson, lie outside the range of matches that might reasonably be expected to be caused by individual variability (Stockman & Sharpe, 2000).

Stockman et al. (1993a) actually used the tritanope data of Wright (1952) to substantially adjust their M- and L-cone fundamentals. Fig. 8 shows the Stockman et al. (1993a) 2° fundamentals determined directly from fits of the Stiles and Burch (1955) 2° CMFs to their spectral sensitivity data (Fig. 1, dotted triangles) before they were adjusted for consistency with Wright's data (shorter dashed line). Any such adjustment, particularly one so large, must be considered to be speculative, since Wright's population was small ($n = 7$), of unknown L- or M-cone genotype, and therefore unlikely to be precisely representative of the normal population. In addition, since Wright's measurements were made with a target of only 1.33° diameter, they are likely to reflect higher underlying photopigment optical densities than the 2° cone fundamentals or CMFs (see Fig. 8 of Stockman & Sharpe, 2000). By contrast, our intermediate 2° cone fundamentals (Fig. 6, open squares), which were also based on fits of the Stiles and Burch (1955) 2° CMFs to spectral sensitivity data (Figs. 3–5), required no adjustments in order to be consistent with the tritan matches.

4. Discussion

The new M- and L-cone spectral sensitivities and the S-cone spectral sensitivities from Stockman et al. (1999) are tabulated in Table 2 of Appendix A for both 2 and 10° diameter targets. The functions are consistent with spectral sensitivities measured in X-chromosome-linked (red–green) dichromats, in S-cone monochromats and in color normals; and they are consistent with tritanopic color matches.

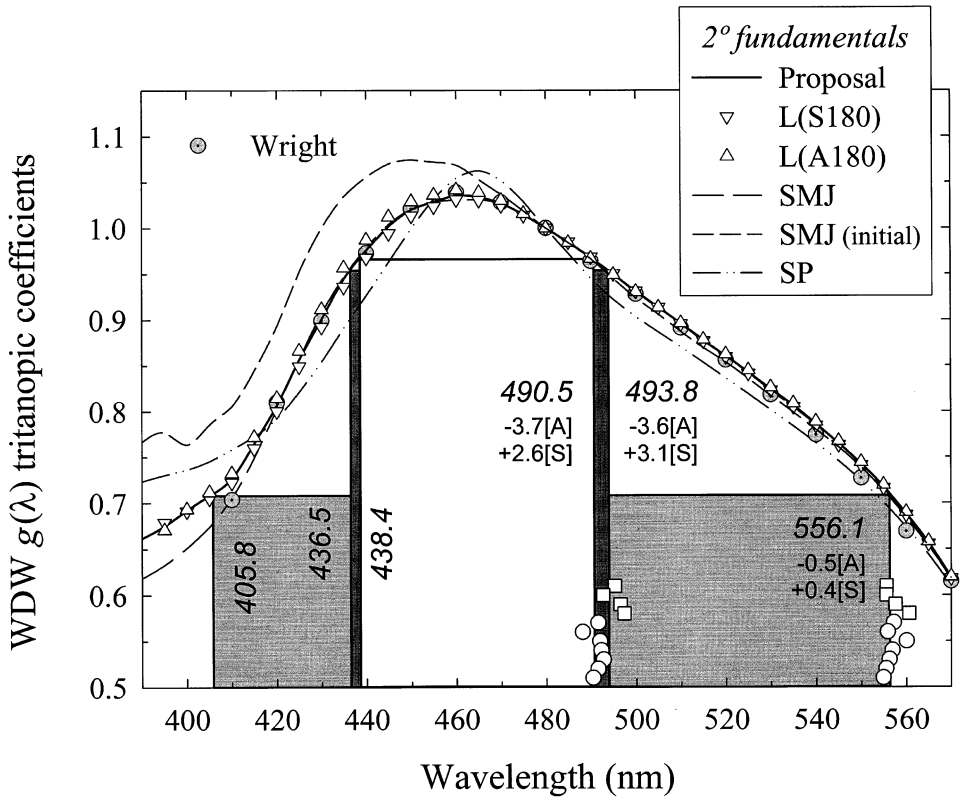

Fig. 8. Tritanopic $g(\lambda)$ predictions of proposed M-cone fundamental and (i) the proposed L-cone fundamental (continuous line, as Fig. 7, diamonds); (ii) the L-cone fundamental with the underlying pigment shifted by 1.46 nm to shorter wavelengths to simulate the L(A180) spectral sensitivity (open triangles); and (iii) the L-cone fundamental shifted by 1.14 nm to longer wavelengths to simulate the L(S180) spectral sensitivity (open inverted triangles). For details, see Stockman and Sharpe (2000). The predicted matches, and the shift in the matches for L(A180) and L(S180) are: 405.8 matches 556.1 nm, -0.5 nm for L(A180) and $+0.4$ nm for L(S180); 436.5 matches 493.8 nm, -3.6 nm for L(A180) and $+3.1$ nm for L(S180); and 438.4 matches 490.5 nm, -3.7 for L(A180) and $+2.6$ nm for L(S180). Also shown are Wright's (1952) tritanopic WDW $g(\lambda)$ coefficients (gray dotted circles), the tritanopic predictions of the Stockman et al. (1993a) M- and L-cone fundamentals before (longer dashed line) and after (shorter dashed line) their adjustment for consistency with Wright's data, and the tritanopic predictions of the Smith and Pokorny M- and L-cone fundamentals (dot-dashed line).

4.1. Previous M- and L-cone fundamentals

Since 1886, several estimates of the normal-cone spectral sensitivities have been based on the loss or reduction hypothesis, notably those by König & Dieterici (1886), Bouma (1942), Judd (1945), Judd (1949), Wyszecki and Stiles (1967), Vos and Walraven (1971), Smith and Pokorny (1975), Estévez (1979), Vos, Estévez and Walraven (1990), and Stockman et al. (1993a).

Fig. 9 shows some of the more recent estimates of the M-cone (a) and L-cone (c) fundamentals by (i) Smith and Pokorny (1975) based on the Judd–Vos modified CIE 1931 2° CMFs (filled circles); (ii) Vos et al. (1990) based on the Stiles and Burch (1955) 2° CMFs (dashed lines); (iii) Stockman et al. (1993a) based on the CIE 1964 10° CMFs corrected to 2° (continuous lines); and (iv) the new estimates tabulated in Table 2 based on the Stiles and Burch (1959) 10° CMFs corrected to 2° (gray dotted circles). The differences between the previous estimates and the new estimate are shown in the corresponding lower panels.

The most discrepant estimate of those shown in Fig. 9 is the M-cone fundamental of Vos et al. (1990), which is too sensitive at longer wavelengths. The reason for this discrepancy is unclear, since Vos et al. (1990) chose their function to be consistent with protanopic spectral sensitivities, but, unlike the other functions, it clearly is not.

While the Smith and Pokorny fundamentals agree with both the Stockman et al. (1993a) and the new fundamentals at middle- and long-wavelengths, they do not agree at short wavelengths. The differences arise mainly because of the insensitivity of Judd–Vos modified CIE 1931 2° CMFs (and the $V(\lambda)$ function) near 460 nm. The agreement with the Smith and Pokorny fundamentals could be improved by large decreases in the macular pigment density of the mean Smith and Pokorny observer, but that would imply that the unadjusted macular pigment density for their observer is implausibly high for a 2° field.

Not surprisingly, given the good agreement between the data on which the two estimates were based (see

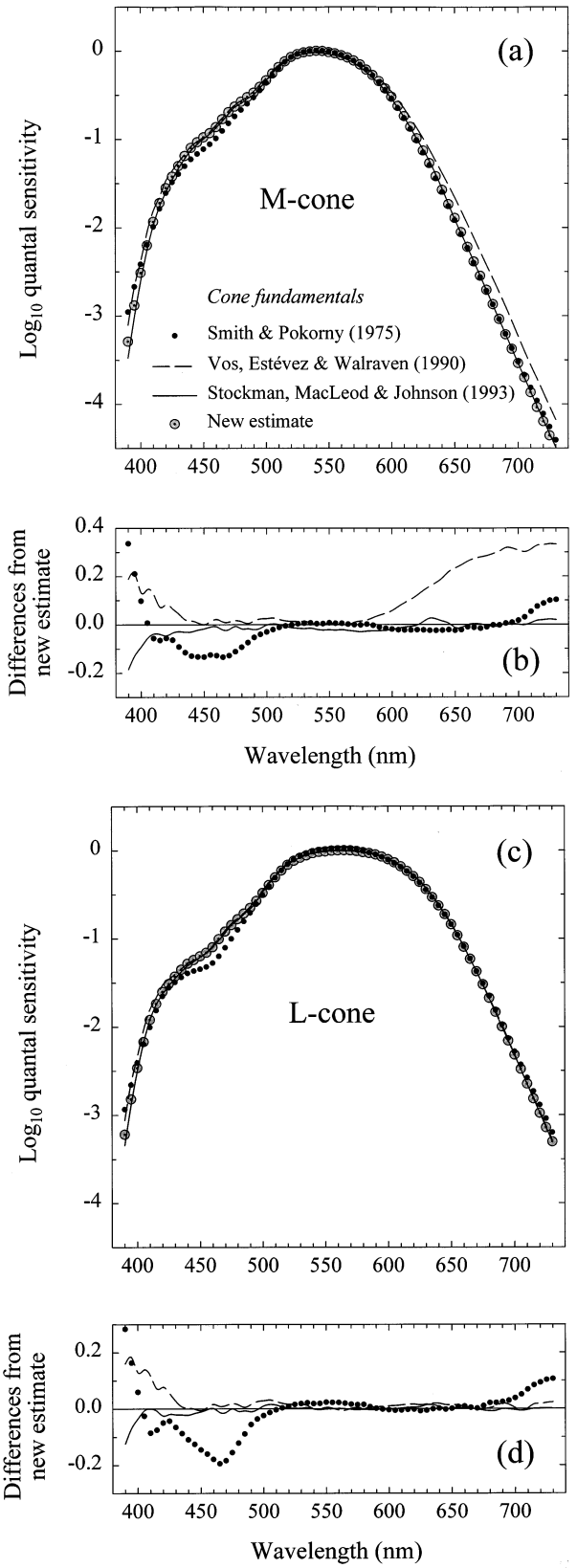

Fig. 9. Estimates of the 2° M- (a) and L- (c) cone fundamentals by Smith and Pokorny (1975) (filled circles); Vos et al. (1990) (dashed lines) and Stockman et al. (1993a) (continuous lines) compared with the new estimates tabulated in Table 2 (gray dotted circles). Differences between the M- (b) and L- (d) cone estimates.

Figs. 1–4), the proposed M- and L-cone fundamentals agree well with those of Stockman et al. (1993a). The discrepancies below 410 nm are mainly the result of adjustments to the Stiles and Burch (1959) CMFs introduced by the CIE to extrapolate the CMFs beyond their measured range, for which there was little or no justification. Differences at short wavelengths also arise because the Stockman et al. (1993a) fundamentals were adjusted for consistency with the 1.33° tritan matches of Wright (1952), which are unlikely to be correct for a 2° target, as evidenced by the discrepancies between those matches and the 2° matches measured by Stockman and Sharpe (2000).

In essence, though, the proposed fundamentals, in the nature of their derivation and their spectral sensitivities, can be considered as a refinement of and improvement upon the Stockman et al. (1993a) fundamentals based on the CIE 1964 10° CMFs corrected to 2°. They incorporate important new molecular genetic and spectral sensitivity data that were unavailable to Stockman, MacLeod and Johnson in 1993.

The differences between the existing S-cone fundamentals and the proposed S-cone fundamental (Table 2) are larger, particularly at middle- and long-wavelengths. Comparisons between the various S-cone fundamentals can be found in Fig. 2.7 of Stockman and Sharpe (1999). For further discussion of the derivation of the S-cone fundamentals tabulated in Table 2, see Stockman et al. (1999).

4.2. Cone spectral sensitivities and luminance

The luminous efficiency function, $V(\lambda)$, is defined as the effectiveness of lights of different wavelength in specific photometric matching tasks. Those tasks now most typically include heterochromatic flicker photometry (HFP), or a version of side-by-side matching, in which the relative intensities of the two half fields are set so that the border between them appears 'minimally distinct' (MDB). Both tasks minimize contributions from the S-cones (see above), and produce nearly additive results (e.g. Ives, 1912; Wagner & Boynton, 1972).

4.2.1. Earlier luminosity functions

The $V(\lambda)$ function, which was adopted by the CIE in 1924 and is still used to define luminance today, was originally proposed by Gibson and Tyndall (1923). The function was based on data obtained using several methods at several laboratories (Ives, 1912; Coblentz & Emerson, 1918; Hyde, Forsythe & Cady, 1918; Gibson & Tyndall, 1923). Surprisingly, the 1924 $V(\lambda)$ function at short wavelengths follows the least plausible data of Hyde, Forsythe and Cady, even though those data are more than a log unit less sensitive than the other data in that region (see Fig. 2.13a of Stockman & Sharpe, 1999).

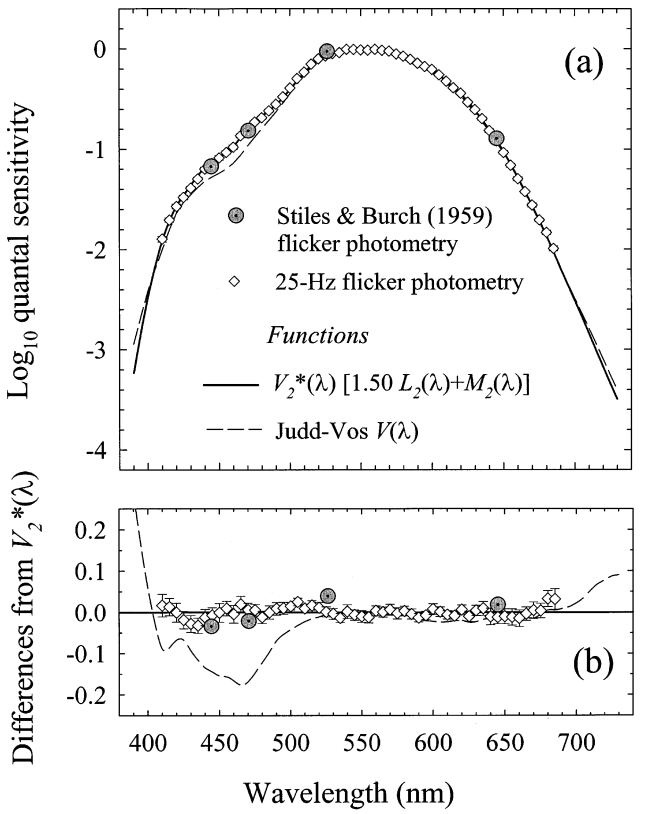

Fig. 10. (a) $V_2^*(\lambda)$ (continuous line), the Judd–Vos modified $V(\lambda)$ (dashed line), mean 25-Hz heterochromatic flicker photometric measurements from 13 L(S180) color normals and 9 L(A180) color normals weighted in the ratio 0.56 L(S180) to 0.44 L(A180) (open diamonds) and used to guide the derivation of $V_2^*(\lambda)$ (Sharpe et al., unpublished observations), and flicker photometric sensitivity measurements by Stiles and Burch (1959) (dotted circles). The weighted 25-Hz HFP mean has been decreased in peak macular pigment density by 0.03 and increased in lens density by 0.26 at 400 nm for best agreement with $V_2^*(\lambda)$. (b) Differences between the $V_2^*(\lambda)$ and the other functions shown in (a).

In 1951, Judd proposed a substantial revision to the $V(\lambda)$ function in an attempt to improve the function at short wavelengths (Judd, 1951). He retained the older photopic sensitivities at 460 nm and longer wavelengths, but increased the sensitivity at shorter wavelengths. Unfortunately, this adjustment artificially created an average observer with an implausibly high macular pigment density for a 2° field. Vos (1978) subsequently made minor adjustments to the Judd modified CIE $V(\lambda)$ function below 410 nm to produce the Judd–Vos modified CIE $V(\lambda)$ (also known as the CIE $V_M(\lambda)$ function), which is shown in Fig. 10 (dashed line).

4.2.2. Cone spectral sensitivities and the luminosity function

The luminosity function, $V(\lambda)$, falls into a completely different category from cone spectral sensitivities, yet it is typically treated as if it did not. Unlike cone spectral sensitivities, the shape of the luminosity function changes with chromatic adaptation (e.g. De Vries, 1948; Eisner & MacLeod, 1981). Thus, any luminosity function is only of limited applicability, since it is not generalizable to other conditions of chromatic adaptation, or necessarily to other measurement tasks. In contrast, cone spectral sensitivities (and CMFs, in general), which are determined by the cone photopigments, do not change with adaptation, until photopigment bleaching becomes significant (in which case, the changes reflect the reduction in photopigment optical density).

Both the M- and the L-cones contribute to luminous efficiency, though their contribution is typically dominated by the L-cones (e.g. Cicerone & Nerger, 1989; Vimal, Smith, Pokorny & Shevell, 1989). The contribution of the S-cones to luminance has been somewhat contentious (Eisner & MacLeod, 1980; Stockman, MacLeod & DePriest, 1987; Verdon & Adams, 1987; Lee & Stromeyer, 1989; Stockman et al., 1991), but it now seems clear that the S-cones do make a small contribution under certain conditions, in particular when the M- and L-cones are selectively adapted to an intense long-wavelength field (Lee & Stromeyer, 1989; Stockman et al., 1991).

Since any small S-cone contribution is not only small, but also strongly temporal-frequency- and adaptation-dependent — to the extent that it might add at some frequencies and subtract at others (Stockman et al., 1991) — it is of practical convenience to treat it as negligible or null; which is the assumption that we make in deriving $V_2^*(\lambda)$, the new luminosity function given below, and that Smith and Pokorny (1975) made in deriving their fundamentals.

4.2.3. $V_2^*(\lambda)$ luminance efficiency function

Unlike the CIE 2° CMFs, the Stiles and Burch 10° (1959) CMFs are purely colorimetric, and are unrelated to any directly measured luminosity function. Given the differences between the CIE and the Stiles and Burch spaces, the CIE $V(\lambda)$ function cannot be used to define luminosity in a Stiles and Burch space without introducing large errors into some calculations (such as in the calculation of the MacLeod–Boynton coordinates from cone spectral sensitivities, see MacLeod & Boynton, 1979). These errors arise in part because of the known problems of the CIE $V(\lambda)$ function (see above), and in part because of the individual differences that inevitably occur between different subject populations.

Instead of $V(\lambda)$, we could use the CIE 1964 estimate of the luminosity function for 10° vision ($\bar{y}_{10}(\lambda)$), which we refer to as $V_{10}(\lambda)$, adjusted to 2°. This function, however, is 'synthetic', since it was constructed from luminosity measurements made at only four wavelengths (see Stiles & Burch, 1959), and anyhow may not be appropriate for 2°. An advantage of the $V_{10}(\lambda)$

function, however, is that it was based in part on data from some of the same subjects used to obtain the Stiles and Burch (1959) 10° CMFs.

To define luminance, we propose a modified $V(\lambda)$ function for 2° observing conditions, which we refer to as $V_2^*(\lambda)$, that retains some of the properties of the original CIE $V(\lambda)$, but is consistent with the new cone fundamentals. One property that is retained, which is also a property of the Smith and Pokorny (1975) cone fundamentals and $V(\lambda)$, is that:

$$V_2^*(\lambda) = a\,\bar{l}_2(\lambda) + \bar{m}_2(\lambda) \quad (6)$$

where a is a scaling constant. The appropriate value of a for the proposed 2° cone fundamentals tabulated in Table 2 could be estimated by finding (i) the linear combination of the 2° fundamentals, $\bar{l}_2(\lambda)$and $\bar{m}_2(\lambda)$, that best fits the CIE Judd–Vos $V(\lambda)$, or (ii) the linear combination of the 10° fundamentals, $\bar{l}_{10}(\lambda)$and $\bar{m}_{10}(\lambda)$ that best fits $V_{10}(\lambda)$, both after best fitting lens and macular pigment adjustments. The best fitting values of a (relative to $\bar{l}(\lambda)$and $\bar{m}(\lambda)$ having the same peak sensitivities) are 1.65 with a standard error of the fitted parameter of 0.15 for the CIE Judd–Vos $V(\lambda)$ and 1.76 with a standard error of 0.05 for $V_{10}(\lambda)$. A concern in using the 10° value of a at 2°, of course, is that a may depend on target size, so that the 10° value is inappropriate at 2°.

We prefer instead to find the linear combination of $\bar{l}_2(\lambda)$and $\bar{m}_2(\lambda)$ that best fits experimentally-determined HFP data. These data, recently obtained in one of our labs for 22 male subjects, 13 of whom were L(S180) and nine of whom were L(A180), were measured using 25-Hz flicker photometry, (see HFP, Section 2). The mean data shown in Fig. 10 (open diamonds) have been weighted so that, like the cone spectral sensitivities (see above), they represent the ratio of 0.56 L(S180) to 0.44 L(A180) found in 304 genotyped individuals (see Table 1) (since the ratio of L(S180) to L(A180) is actually 0.59:0.41 for our 22 subjects, the change from the unweighted mean is minimal). After macular and lens adjustments, the best fitting value of a is 1.50 with a standard error of the fitted parameter of 0.06, and the rms error is an impressively small 0.013 log unit (which attests to the predictive qualities of the cone fundamentals)[2]. Based on the experimental data, the value of a is therefore 1.50, and the definition of $V_2^*(\lambda)$ is:

$$V_2^*(\lambda) = 1.50\,\bar{l}_2(\lambda) + \bar{m}_2(\lambda) \quad (7)$$

again relative to $\bar{l}_2(\lambda)$and $\bar{m}_2(\lambda)$ having the same peak sensitivities. $V_2^*(\lambda)$ is tabulated in Table 2. A value of 1.62 is implied by the relationship of the Smith and Pokorny L- and M-cone fundamentals to the Judd–Vos $V(\lambda)$.

Fig. 10a shows $V_2^*(\lambda)$ (continuous line) and the Judd–Vos $V(\lambda)$ (dashed line) functions, and Fig. 10b the differences between them. The 2° flicker photometric measurements made at four wavelengths in 26 of the 49 observers of the Stiles and Burch (1959) 10° color matching study, which are shown as the dotted circles, are also clearly closer to $V_2^*(\lambda)$.

4.3. Direct methods of determining photopigment spectra

Two methods have yielded human photopigment spectra that have frequently been compared with corneally-measured spectral sensitivity functions: microspectrophotometry (MSP) and suction electrode recordings.

4.3.1. MSP

In MSP work, the spectral transmission of a small measuring beam passed transversely through the outer segment of a single cone is compared with that of a reference beam passed outside the cone to derive the absorption spectrum of the outer segment (e.g. Bowmaker, Dartnall, Lythgoe & Mollon, 1978). Of particular interest here are the human MSP measurements of Dartnall, Bowmaker and Mollon (1983) of photoreceptors 'from the eyes of seven persons.'

Fig. 11a compares the S- (white squares), M- (gray diamonds) and L- (black circles) cone MSP results with the photopigment optical density spectra (continuous lines) tabulated in Table 2. As Fig. 11a makes clear, MSP is of little use in defining cone spectral sensitivities except close to the photopigment λ_{max}. The large discrepancies between MSP and other estimates of cone spectral sensitivities arise because of the small signal to noise ratio of the MSP measurements. MSP is, nonetheless, useful for defining photopigment λ_{max}. From their MSP measurements, Dartnall et al. (1983) estimated the human photopigment λ_{max} wavelengths to be 419.0 nm (S-cone), 530.8 nm (M-cone) and 558.4 nm (L-cone). These agree extremely well with the λ_{max} estimates of 420.7 (S-cone), 530.3 (M-cone) and 558.9 nm (L-cone) obtained by fitting the template (Eq. (8), see below) to the photopigment spectra tabulated in Table 2.

4.3.2. Suction electrode recordings

In suction electrode recordings, a single photoreceptor outer segment is drawn inside a small glass electrode, and its current response to light is recorded (e.g. Baylor, Nunn & Schnapf, 1984, 1987). Spectral sensitivity is obtained by finding, as a function of wavelength, the radiance required to elicit a criterion photocurrent response.

[2] If an S-cone contribution is allowed, the S-cone weight is negative, and is only 0.98% of the L-cone weight. Since different populations are being compared, we cannot be certain whether such a small contribution is real or due to other factors, such as noise or sources of individual variability that we have not accounted for.

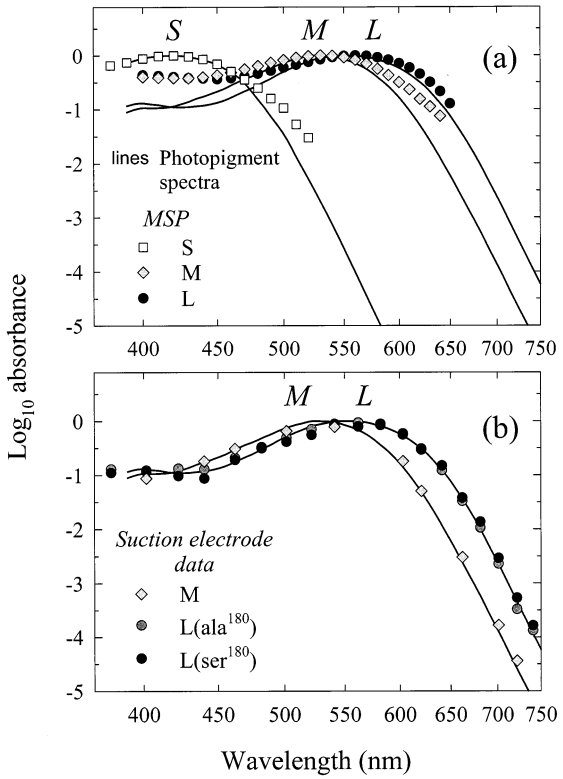

Fig. 11. Log_{10} S-, M- and L-cone photopigment spectra calculated from the new cone fundamentals (continuous lines) compared with (a) human S- (white squares), M- (gray diamonds) and L- (black circles) cone MSP measurements by Dartnall et al. (1983) and (b) human M-cone (gray diamonds) suction electrode measurements by Kraft (personal communication), and L(A180)-cone (gray circles) and L(S180)-cone (black circles) suction electrode measurements by Kraft et al. (1998).

Relevant human suction electrode data have so far been obtained only from M- and L-cones (Schnapf, Kraft & Baylor, 1987; Kraft, Neitz & Neitz, 1998). Recently, Kraft et al. (1998) have made measurements in human L-cones known to contain photopigments that are determined either by L(S180) or by L(A180) genes, and Kraft (personal communication) has made measurements in human M-cones. Their M (gray diamonds), L(A180) (gray circles) and L(S180) (black circles) data are shown in Fig. 11b along with the photopigment spectra from Table 2 (lines).

Given that no attempt has been made to improve the agreement between the two data sets, the agreement, particularly at shorter wavelengths, is good. At longer wavelengths, the L(A180) suction electrode data agree well with the corneally-derived L-cone photopigment spectra, but the M and L(S180) suction electrode data are slightly shallower than the corneally-derived M- and L-cone functions. Such differences have been encountered before, but have been minimized by assuming unusually low peak photopigment optical densities for the central 2° of vision (Baylor et al., 1987) or by comparing them with corneally-measured spectral sensitivities that are implausibly shallow at longer wavelengths (Nunn, Schnapf & Baylor, 1984; Baylor et al., 1987). In fact, the differences might be consistent with waveguiding, since in both microspectrophotometry and suction electrode recordings, the spectral sensitivity of the photopigment is measured transversely across the isolated cone outer segment, rather than axially along the outer segment as in normal vision.

Light is transmitted along the photoreceptor in patterns called waveguide modal patterns (see Fig. 6 of Enoch, 1963). The fraction of the power of each modal pattern that is transmitted inside the photoreceptor to its power outside the photoreceptor decreases with the wavelength of the incident light, so that, in principle, the structure of the photoreceptor can change its spectral sensitivity (see, for example, Enoch, 1961; Enoch & Stiles, 1961; Snyder, 1975; Horowitz, 1981). Given values of 1μm for the diameter of a human foveal-cone outer segment (Polyak, 1941), and 1.39 and 1.35, respectively, for the refractive indices inside and outside the cone outer segment (Fig. 6.11 of Horowitz, 1981), standard formulae (Eq. 7a and Fig. 9 of Snyder, 1975) suggest a loss of spectral sensitivity for mode η_{11} (the most important mode for axially incident light) of about 0.2 $\log_{10}$ unit for red light relative to violet. Waveguide effects of this magnitude could explain the differences between the suction electrode data and photopigment optical density spectra shown in Fig. 11b.

4.4. Photopigment nomograms or templates

Attempts have been made to simplify photopigment optical density spectra by finding an abscissa that yields photopigment optical density spectra of fixed spectral shape, whatever their λ_{max}. An early proposal by Dartnall (1953) was for a 'nomogram' or fixed template shape for photopigment spectra plotted as a function of wavenumber ($1/\lambda$, in units of cm^{-1}). Later, Barlow (1982) proposed that an abscissa of the fourth root of wavelength ($\sqrt[4]{\lambda}$) produced invariant photopigment spectra. A more recent proposal was that photopigment spectra are invariant when plotted as a function of $\log_{10}$ frequency ($\log_{10}(1/\lambda)$) (Mansfield, 1985; MacNichol, 1986), which is equivalent to $\log_{10}$ wavelength ($\log_{10}(\lambda)$) or normalized frequency (λ/λ_{max}).

Fig. 12 shows the new S- (white squares), M- (gray diamonds) and L- (black circles) cone photopigment optical density spectra calculated from the new cone fundamentals and tabulated in Table 2. They are plotted against a log wavelength scale, for which Lamb (1995) has proposed a standard template shape to characterize the shape of the photopigment spectra near their peak sensitivity and at longer wavelengths.

Fig. 12a shows the Lamb template (continuous lines) fitted to each of the log S-, M- and L-cone photopig-

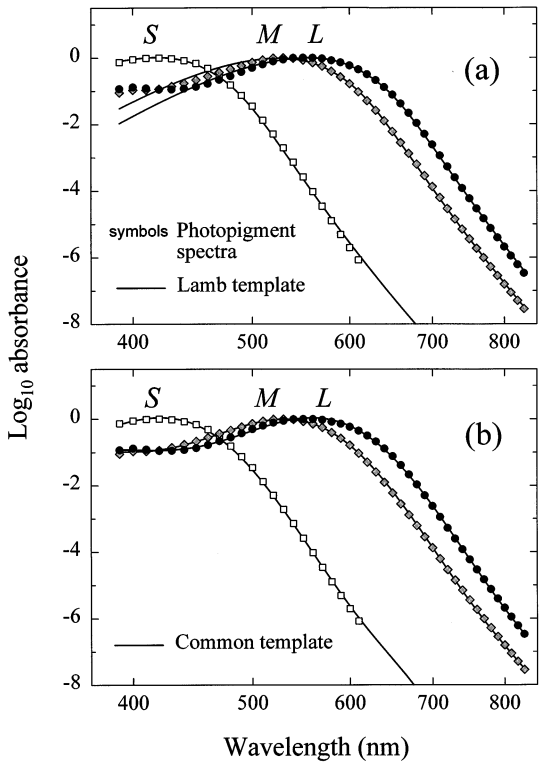

Fig. 12. Log_{10} S- (white squares), M- (gray diamonds) and L- (black circles) cone photopigment spectra calculated from the new cone fundamentals and (a) longer wavelength fits of the Lamb (1995) template with λ_{max} values of 418.1, 526.2 and 555.7 nm (continuous lines) or (b) fits of the template defined by Eq. (8) with λ_{max} values of 420.7, 530.3 and 558.9 nm (continuous lines). For clarity, the photopigment density spectra are plotted at only 10-nm intervals.

ment spectra at wavelengths from 20 nm shorter than the λ_{max} to long wavelengths by minimizing the squared deviations between the template and the spectra. Wavelengths more than 20 nm shorter than the λ_{max} fit the template poorly, and so distort the template fit at longer wavelengths. The λ_{max} values of the fitted templates are 418.1, 526.2 and 555.7 nm for S-, M- and L-cones, respectively. Lamb's function is adequate at longer wavelengths, but does a poor job of characterizing the shorter wavelength portions of the photopigment spectra — a problem noted by Lamb (1995) himself.

Because there is interest in having a template that approximates the photopigment spectra over the entire range of visible wavelengths, we have derived a common or average template for the three photopigment optical density spectra (t_{OD}) for the log wavelength scale. It is:

$$\log_{10}[t_{OD}(x)] = a + b\,x^2 + c\,x^4 + d\,x^6 + e\,x^8 + f\,x^{10} + g\,x^{12} + h\,x^{14} \quad (8)$$

where x is $\log_{10}$ (nm), $a = -188862.970810906644$, $b = 90228.966712600282$, $c = -2483.531554344362$, $d = -6675.007923501414$, $e = 1813.525992411163$, $f = -215.177888526334$, $g = 12.487558618387$, and $h = -0.289541500599$.

The function was obtained iteratively. First, a polynomial was derived to describe the L-cone log photopigment optical density spectra plotted as a function of log wavelength (using TableCurve 2D, SPSS, Chicago). Second, the S-, M- and L-cone log optical density spectra were shifted along a log wavelength axis to best least-squares fit the polynomial (a small vertical shift was also allowed). Next, a second polynomial was derived to describe *all three* shifted cone optical density spectra. The last two steps were repeated until there was no improvement in the least-squares fit over the previous fit. Different starting templates were tried, but with little effect on the final solution.

The final template function defined by Eq. (8) (which peaks at 558.0 nm) has been fitted (continuous lines) to each of the S-, M- and L-cone photopigment spectra shown in Fig. 12b by shifting it horizontally along a log wavelength scale and minimizing the squared deviations between the template and the spectra. The λ_{max} values of the fitted templates are 420.7, 530.3 and 558.9 nm for S-, M- and L-cones, respectively; and the rms error is 0.030. There are slight deviations from the common shape, particularly in the case of the S-cone spectrum. Nonetheless, the overall agreement is good, the template providing a reasonable approximation to the measured spectra, and a better approximation than the Lamb template at short wavelengths.

We also derived templates using the same iterative procedure for a wavenumber and for a fourth root of wavelength scale. The fits and rms errors were substantially worse. For the wavenumber ($1/\lambda$) scale, the rms error was 0.129, while for the fourth root of wavelength scale ($\sqrt[4]{\lambda}$), it was 0.056. Visual inspection also confirmed that of the three scales the photopigment optical density spectra are most similar in shape when plotted against a log wavelength scale.

The λ_{max} estimates for the S-, M- and L-cones obtained with Eq. (8) are 2.7, 4.6 and 3.4 nm longer, respectively, than those obtained with the Lamb template. These discrepancies arise because Lamb's template is slightly more sensitive than both Eq. (8) and the data at wavelengths just short of the λ_{max} (before becoming implausible at still shorter wavelengths). Lamb's formula was derived by amalgamating the results of many studies. It may be that the human cone photopigment spectra measured axially along the cone outer segment differ in shape from other measurements of photopigment spectra. Or it may be that basing a template on data from many studies differing in technique and precision unavoidably introduces error.

Eq. (8) is useful from 0.155 $\log_{10}$ nm below the photopigment λ_{max} to 0.195 $\log_{10}$ nm above it (e.g. for the L-cone photopigment from 390 to 875 nm), which covers a sensitivity range at wavelengths longer than

the λ_{max} of 7.5 $\log_{10}$ units. Outside this range, the function deviates from the shapes of known photopigment spectra. Marginally better fits to the photopigment spectra can be obtained with functions of higher order (e.g. Chebyshev, Fourier series, or simple polynomials), but the improvement is slight (rms errors of ~ 0.028 vs 0.030).

Although the photopigment optical density spectra are approximately shape invariant when plotted as a function of log wavelength, it should be recognized that some factors make shape invariance unlikely. Waveguiding, for example, acts, in part, like interposing a filter with fixed spectral properties in front of the photopigments, thus altering the photopigment spectra differently according to their λ_{max} and causing shape invariance to fail.

Acknowledgements

Supported by National Institutes of Health grant EY 10206 awarded to AS, and by the Deutsche Forschungsgemeinschaft (Bonn) grants SFB 325 Tp A13 and Sh23/5-1 and a Hermann- und Lilly-Schilling-Stiftung-Professur awarded to LTS. We thank Jeremy Nathans for the molecular genetic analyses of the dichromats, Timothy Kraft for providing the suction electrode data, Rhea Eskew for contributions to the luminance section, and Donald MacLeod for valuable and timely insights. We are especially grateful to an anonymous reviewer who helped us to clarify and improve several aspects of our analysis.

Appendix A

A.1. New fundamentals

In Table 2, we present a consistent set of functions: the quantal 2° cone fundamentals $\bar{l}_2(\lambda)$ (L-cone), $\bar{m}_2(\lambda)$ (M-cone) and $\bar{s}_2(\lambda)$ (S-cone); the quantal 2° luminous efficiency function, $V_2^*(\lambda)$; the quantal 10° cone fundamentals $\bar{l}_{10}(\lambda)$, $\bar{m}_{10}(\lambda)$ and $\bar{s}_{10}(\lambda)$; the three photopigment optical densities, $\bar{l}_{OD}(\lambda)$, $\bar{m}_{OD}(\lambda)$ and $\bar{s}_{OD}(\lambda)$; the lens density spectrum, $d_{lens}(\lambda)$; and the macular pigment density spectrum, $d_{mac}(\lambda)$, tabulated for the central 2° (the 10° macular pigment densities are 0.2714 times these values). Together these can be used to define normal human color vision.

A.2. Stiles and Burch 10° color matching functions

The Stiles and Burch (1959) 10° CMFs used to calculate the cone fundamentals are tabulated in Table 3 in energy units. To achieve the necessary precision at longer wavelengths to define the cone fundamentals, we have reinterpolated the original color matching functions at 5-nm steps, after making the corrections for rod intrusion given by Stiles and Burch in their Table 8.

The data contained in Tables 2 and 3 are available on our Web sites:
http://www-cvrl.ucsd.edu (America)
http://www.eye.medizin.uni-tuebingen.de/cvrl (Germany), where they can be found tabulated in 0.1, 1 and 5-nm steps. Please check these sites for updates and corrections.

Table 2
Proposed quantal 2° cone spectral sensitivities: log $L_2(\lambda)$ or log $\bar{l}_2(\lambda)$, log $M_2(\lambda)$ or log $\bar{m}_2(\lambda)$ and log $S_2(\lambda)$ or log $\bar{s}_2(\lambda)$; quantal 2° luminosity function: log $V_2^*(\lambda)$; quantal 10° cone spectral sensitivities: log $L_{10}(\lambda)$ or log $\bar{l}_{10}(\lambda)$, log $M_{10}(\lambda)$ or log $\bar{m}_{10}(\lambda)$ and log $S_{10}(\lambda)$ or log $\bar{s}_{10}(\lambda)$; photopigment optical densities: log $\bar{l}_{OD}(\lambda)$, log $\bar{m}_{OD}(\lambda)$ and log $\bar{s}_{OD}(\lambda)$; and the lens and 2° macular pigment density spectra: $d_{lens}(\lambda)$and $d_{mac}(\lambda)$[a,b,c,d,e]

λ (nm)	Log $L_2(\lambda)$ (log $\bar{l}_2(\lambda)$)	Log $M_2(\lambda)$ (log $\bar{m}_2(\lambda)$)	Log $S_2(\lambda)$ (log $\bar{s}_2(\lambda)$)	Log $V_2^*(\lambda)$	Log $L_{10}(\lambda)$ (log $\bar{l}_{10}(\lambda)$)	Log $M_{10}(\lambda)$ (log $\bar{m}_{10}(\lambda)$)	Log $S_{10}(\lambda)$ (log $\bar{s}_{10}(\lambda)$)	Log $\bar{l}_{OD}(\lambda)$	Log $\bar{m}_{OD}(\lambda)$	Log $\bar{s}_{OD}(\lambda)$	Lens ($d_{lens}(\lambda)$)	Macular$_2$ $d_{mac}(\lambda)$)
390	−3.2186	−3.2908	−1.9660	−3.2335	−3.2275	−3.3041	−2.1520	−0.9338	−1.0479	−0.1339	2.5122	0.0453
395	−2.8202	−2.8809	−1.5744	−2.8310	−2.8142	−2.8793	−1.7431	−0.8948	−0.9974	−0.0908	2.1306	0.0649
400	−2.4660	−2.5120	−1.2037	−2.4713	−2.4438	−2.4941	−1.3533	−0.8835	−0.9707	−0.0499	1.7649	0.0868
405	−2.1688	−2.2013	−0.8743	−2.1690	−2.1286	−2.1651	−1.0036	−0.9016	−0.9742	−0.0258	1.4257	0.1120
410	−1.9178	−1.9346	−0.6002	−1.9119	−1.8599	−1.8804	−0.7104	−0.9154	−0.9711	−0.0093	1.1374	0.1365
415	−1.7371	−1.7218	−0.3915	−1.7184	−1.6602	−1.6482	−0.4817	−0.9408	−0.9623	−0.0024	0.9063	0.1631
420	−1.6029	−1.5535	−0.2427	−1.5699	−1.5008	−1.4540	−0.3072	−0.9549	−0.9398	0.0000	0.7240	0.1981
425	−1.5136	−1.4235	−0.1542	−1.4627	−1.3849	−1.2968	−0.1926	−0.9576	−0.8990	−0.0055	0.5957	0.2345
430	−1.4290	−1.3033	−0.0838	−1.3618	−1.2804	−1.1560	−0.1037	−0.9536	−0.8564	−0.0222	0.4876	0.2618
435	−1.3513	−1.1900	−0.0373	−1.2669	−1.1913	−1.0304	−0.0483	−0.9390	−0.8027	−0.0500	0.4081	0.2772
440	−1.2842	−1.0980	−0.0022	−1.1874	−1.1159	−0.9294	−0.0073	−0.9267	−0.7627	−0.0811	0.3413	0.2884
445	−1.2414	−1.0342	−0.0069	−1.1338	−1.0583	−0.8502	0.0005	−0.9041	−0.7159	−0.1201	0.3000	0.3080
450	−1.2010	−0.9794	−0.0278	−1.0860	−0.9991	−0.7758	−0.0063	−0.8734	−0.6675	−0.1667	0.2629	0.3332
455	−1.1606	−0.9319	−0.0782	−1.0418	−0.9467	−0.7156	−0.0498	−0.8335	−0.6174	−0.2398	0.2438	0.3486
460	−1.0974	−0.8632	−0.1217	−0.9757	−0.8814	−0.6439	−0.0963	−0.7801	−0.5543	−0.3146	0.2279	0.3500
465	−1.0062	−0.7734	−0.1540	−0.8853	−0.8058	−0.5686	−0.1492	−0.7211	−0.4924	−0.4012	0.2131	0.3269
470	−0.9200	−0.6928	−0.2164	−0.8020	−0.7379	−0.5056	−0.2357	−0.6643	−0.4374	−0.5169	0.2046	0.2996
475	−0.8475	−0.6301	−0.3185	−0.7346	−0.6751	−0.4520	−0.3531	−0.6122	−0.3925	−0.6627	0.1929	0.2842
480	−0.7803	−0.5747	−0.4446	−0.6736	−0.6100	−0.3981	−0.4863	−0.5515	−0.3405	−0.8166	0.1834	0.2786
485	−0.7166	−0.5235	−0.5777	−0.6163	−0.5449	−0.3447	−0.6226	−0.4871	−0.2850	−0.9683	0.1749	0.2772
490	−0.6535	−0.4738	−0.7189	−0.5600	−0.4854	−0.2982	−0.7716	−0.4289	−0.2378	−1.1321	0.1675	0.2688
495	−0.5730	−0.4078	−0.8439	−0.4867	−0.4165	−0.2433	−0.9124	−0.3618	−0.1821	−1.2892	0.1601	0.2485
500	−0.4837	−0.3337	−0.9644	−0.4049	−0.3527	−0.1945	−1.0624	−0.3040	−0.1384	−1.4586	0.1537	0.2093
505	−0.3929	−0.2569	−1.1092	−0.3208	−0.2907	−0.1467	−1.2399	−0.2499	−0.0980	−1.6574	0.1463	0.1652
510	−0.3061	−0.1843	−1.2783	−0.2407	−0.2328	−0.1034	−1.4416	−0.2007	−0.0644	−1.8809	0.1378	0.1211
515	−0.2279	−0.1209	−1.4350	−0.1694	−0.1804	−0.0668	−1.6276	−0.1559	−0.0383	−2.0870	0.1293	0.0812
520	−0.1633	−0.0699	−1.6054	−0.1110	−0.1332	−0.0341	−1.8190	−0.1094	−0.0095	−2.2930	0.1230	0.0525
525	−0.1178	−0.0389	−1.7873	−0.0720	−0.0993	−0.0165	−2.0154	−0.0771	0.0000	−2.5013	0.1166	0.0329
530	−0.0830	−0.0191	−1.9787	−0.0438	−0.0739	−0.0083	−2.2180	−0.0550	−0.0037	−2.7146	0.1102	0.0175
535	−0.0571	−0.0081	−2.1750	−0.0243	−0.0521	−0.0036	−2.4203	−0.0332	−0.0082	−2.9246	0.1049	0.0093
540	−0.0330	−0.0004	−2.3806	−0.0072	−0.0292	0.0000	−2.6293	−0.0095	−0.0146	−3.1413	0.0986	0.0046
545	−0.0187	−0.0036	−2.5903	0.0001	−0.0161	−0.0073	−2.8412	0.0000	−0.0370	−3.3604	0.0922	0.0017
550	−0.0128	−0.0163	−2.8031	−0.0017	−0.0118	−0.0244	−3.0553	−0.0040	−0.0731	−3.5813	0.0859	0.0000
555	−0.0050	−0.0295	−3.0189	−0.0022	−0.0039	−0.0402	−3.2711	−0.0014	−0.1055	−3.8035	0.0795	0.0000
560	−0.0019	−0.0514	−3.2336	−0.0085	−0.0011	−0.0655	−3.4858	−0.0055	−0.1485	−4.0235	0.0742	0.0000
565	−0.0001	−0.0769	−3.4479	−0.0167	0.0000	−0.0944	−3.7001	−0.0138	−0.1966	−4.2442	0.0678	0.0000
570	−0.0015	−0.1115	−3.6607	−0.0297	−0.0027	−0.1329	−3.9129	−0.0280	−0.2554	−4.4633	0.0615	0.0000
575	−0.0086	−0.1562	−3.8713	−0.0493	−0.0120	−0.1817	−4.1235	−0.0519	−0.3251	−4.6803	0.0551	0.0000
580	−0.0225	−0.2143	−4.0790	−0.0769	−0.0288	−0.2440	−4.3312	−0.0863	−0.4084	−4.8943	0.0488	0.0000
585	−0.0325	−0.2753	−4.2831	−0.1016	−0.0408	−0.3085	−4.5353	−0.1113	−0.4903	−5.1038	0.0435	0.0000
590	−0.0491	−0.3443	−4.4832	−0.1320	−0.0600	−0.3808	−4.7353	−0.1460	−0.5788	−5.3091	0.0381	0.0000
595	−0.0727	−0.4264	−4.6787	−0.1697	−0.0869	−0.4659	−4.9309	−0.1898	−0.6791	−5.5100	0.0329	0.0000

Table 2 (*Continued*)

λ (nm)	Log $L_2(\lambda)$ (log $\bar{l}_2(\lambda)$)	Log $M_2(\lambda)$ (log $\bar{m}_2(\lambda)$)	Log $S_2(\lambda)$ (log $\bar{s}_2(\lambda)$)	Log $V_2^*(\lambda)$	Log $L_{10}(\lambda)$ (log $\bar{l}_{10}(\lambda)$)	Log $M_{10}(\lambda)$ (log $\bar{m}_{10}(\lambda)$)	Log $S_{10}(\lambda)$ (log $\bar{s}_{10}(\lambda)$)	Log $\bar{l}_{OD}(\lambda)$	Log $\bar{m}_{OD}(\lambda)$	Log $\bar{s}_{OD}(\lambda)$	Lens ($d_{lens}(\lambda)$)	Macular$_2$ $d_{mac}(\lambda)$)
600	−0.1026	−0.5198	−4.8694	−0.2133	−0.1200	−0.5619	−5.1216	−0.2378	−0.7868	−5.7038	0.0297	0.0000
605	−0.1380	−0.6247	−5.0550	−0.2619	−0.1588	−0.6690	−5.3071	−0.2929	−0.9054	−5.8936	0.0254	0.0000
610	−0.1823	−0.7390	−5.2351	−0.3179	−0.2066	−0.7851	−5.4873	−0.3561	−1.0305	−6.0770	0.0223	0.0000
615	−0.2346	−0.8610	−5.4098	−0.3804	−0.2623	−0.9086	−5.6620	−0.4268	−1.1617	−6.2548	0.0191	0.0000
620	−0.2943	−0.9915	–	−0.4491	−0.3252	−1.0401	–	−0.5026	−1.2989	–	0.0170	0.0000
625	−0.3603	−1.1294	–	−0.5230	−0.3940	−1.1789	–	−0.5833	−1.4425	–	0.0148	0.0000
630	−0.4421	−1.2721	–	−0.6106	−0.4788	−1.3222	–	−0.6809	−1.5909	–	0.0117	0.0000
635	−0.5327	−1.4205	–	−0.7061	−0.5718	−1.4710	–	−0.7854	−1.7444	–	0.0085	0.0000
640	−0.6273	−1.5748	–	−0.8051	−0.6684	−1.6257	–	−0.8918	−1.9033	–	0.0053	0.0000
645	−0.7262	−1.7370	–	−0.9082	−0.7690	−1.7881	–	−0.9986	−2.0675	–	0.0042	0.0000
650	−0.8407	−1.8900	–	−1.0249	−0.8849	−1.9413	–	−1.1202	−2.2222	–	0.0032	0.0000
655	−0.9658	−2.0523	–	−1.1521	−1.0112	−2.1037	–	−1.2523	−2.3871	–	0.0011	0.0000
660	−1.0966	−2.2220	–	−1.2848	−1.1429	−2.2735	–	−1.3879	−2.5582	–	0.0000	0.0000
665	−1.2327	−2.3923	–	−1.4224	−1.2796	−2.4438	–	−1.5268	−2.7287	–	0.0000	0.0000
670	−1.3739	−2.5559	–	−1.5646	−1.4213	−2.6074	–	−1.6700	−2.8924	–	0.0000	0.0000
675	−1.5208	−2.7194	–	−1.7121	−1.5686	−2.7709	–	−1.8185	−3.0560	–	0.0000	0.0000
680	−1.6736	−2.8843	–	−1.8655	−1.7217	−2.9359	–	−1.9725	−3.2210	–	0.0000	0.0000
685	−1.8328	−3.0519	–	−2.0250	−1.8811	−3.1035	–	−2.1325	−3.3887	–	0.0000	0.0000
690	−1.9992	−3.2234	–	−2.1916	−2.0476	−3.2750	–	−2.2994	−3.5602	–	0.0000	0.0000
695	−2.1596	−3.3874	–	−2.3522	−2.2081	−3.4390	–	−2.4603	−3.7242	–	0.0000	0.0000
700	−2.3200	−3.5484	–	−2.5126	−2.3686	−3.6000	–	−2.6209	−3.8852	–	0.0000	0.0000
705	−2.4819	−3.7103	–	−2.6745	−2.5306	−3.7619	–	−2.7830	−4.0472	–	0.0000	0.0000
710	−2.6490	−3.8757	–	−2.8415	−2.6977	−3.9273	–	−2.9502	−4.2125	–	0.0000	0.0000
715	−2.8165	−4.0389	–	−3.0088	−2.8651	−4.0905	–	−3.1178	−4.3757	–	0.0000	0.0000
720	−2.9801	−4.1981	–	−3.1723	−3.0288	−4.2497	–	−3.2815	−4.5350	–	0.0000	0.0000
725	−3.1432	−4.3559	–	−3.3352	−3.1919	−4.4075	–	−3.4446	−4.6928	–	0.0000	0.0000
730	−3.3032	−4.5101	–	−3.4949	−3.3519	−4.5618	–	−3.6046	−4.8470	–	0.0000	0.0000
735	−3.4625	−4.6634	–	−3.6540	−3.5112	−4.7150	–	−3.7640	−5.0002	–	0.0000	0.0000
740	−3.6223	−4.8153	–	−3.8134	−3.6710	−4.8669	–	−3.9237	−5.1522	–	0.0000	0.0000
745	−3.7767	−4.9607	–	−3.9675	−3.8254	−5.0123	–	−4.0781	−5.2976	–	0.0000	0.0000
750	−3.9316	−5.1068	–	−4.1220	−3.9803	−5.1584	–	−4.2331	−5.4437	–	0.0000	0.0000
755	−4.0841	−5.2505	–	−4.2742	−4.1328	−5.3022	–	−4.3856	−5.5874	–	0.0000	0.0000
760	−4.2344	−5.3916	–	−4.4240	−4.2831	−5.4432	–	−4.5359	−5.7285	–	0.0000	0.0000
765	−4.3840	−5.5326	–	−4.5732	−4.4327	−5.5842	–	−4.6855	−5.8695	–	0.0000	0.0000
770	−4.5308	−5.6715	–	−4.7197	−4.5795	−5.7231	–	−4.8323	−6.0083	–	0.0000	0.0000
775	−4.6783	−5.8107	–	−4.8668	−4.7270	−5.8623	–	−4.9798	−6.1475	–	0.0000	0.0000
780	−4.8211	−5.9447	–	−5.0091	−4.8698	−5.9963	–	−5.1226	−6.2816	–	0.0000	0.0000
785	−4.9631	−6.0778	–	−5.1508	−5.0119	−6.1295	–	−5.2646	−6.4147	–	0.0000	0.0000
790	−5.1040	−6.2097	–	−5.2913	−5.1527	−6.2614	–	−5.4055	−6.5466	–	0.0000	0.0000
795	−5.2441	−6.3405	–	−5.4309	−5.2928	−6.3921	–	−5.5456	−6.6774	–	0.0000	0.0000
800	−5.3815	−6.4673	–	−5.5677	−5.4302	−6.5189	–	−5.6830	−6.8042	–	0.0000	0.0000
805	−5.5168	−6.5919	–	−5.7025	−5.5655	−6.6435	–	−5.8183	−6.9288	–	0.0000	0.0000
810	−5.6530	−6.7176	–	−5.8381	−5.7017	−6.7692	–	−5.9545	−7.0544	–	0.0000	0.0000
815	−5.7867	−6.8409	–	−5.9712	−5.8354	−6.8925	–	−6.0882	−7.1778	–	0.0000	0.0000

Table 2 (*Continued*)

λ (nm)	Log $L_2(\lambda)$ (log $\bar{l}_2(\lambda)$)	Log $M_2(\lambda)$ (log $\bar{m}_2(\lambda)$)	Log $S_2(\lambda)$ (log $\bar{s}_2(\lambda)$)	Log $V_2^*(\lambda)$	Log $L_{10}(\lambda)$ (log $\bar{l}_{10}(\lambda)$)	Log $M_{10}(\lambda)$ (log $\bar{m}_{10}(\lambda)$)	Log $S_{10}(\lambda)$ (log $\bar{s}_{10}(\lambda)$)	Log $\bar{l}_{OD}(\lambda)$	Log $\bar{m}_{OD}(\lambda)$	Log $\bar{s}_{OD}(\lambda)$	Lens ($d_{lens}(\lambda)$)	Macular$_2$ $d_{mac}(\lambda)$)
820	−5.9172	−6.9619	–	−6.1012	−5.9659	−7.0135	–	−6.2187	−7.2987	–	0.0000	0.0000
825	−6.0473	−7.0837	–	−6.2308	−6.0960	−7.1354	–	−6.3488	−7.4206	–	0.0000	0.0000
830	−6.1760	−7.2058	–	−6.3591	−6.2247	−7.2574	–	−6.4775	−7.5426	–	0.0000	0.0000

[a] To convert quantal units to energy units add log(λ) and renormalize.

[b] The cone spectral sensitivities and the luminosity function are normalized to unity peaks, which were estimated to the nearest 0.1 nm from the 5-nm values by cubic spline interpolation. $V_2^*(\lambda) = 1.50\ L_2(\lambda) + M_2(\lambda)$.

[c] The cone fundamentals were calculated using the Stiles and Burch (1959) 10° CMFs using $\bar{s}_G/\bar{s}_B = 0.010600$ for S; $\bar{m}_R/\bar{m}_B = 0.168926$ and $\bar{m}_G/\bar{m}_B = 8.265895$ for M and $\bar{l}_R/\bar{l}_B = 2.846201$ and $\bar{l}_G/\bar{l}_B = 11.092490$ for L. For further details about the long-wavelength S-cone extension after 520 nm, see Stockman et al. (1999). Stockman et al. (1999) were unable to measure S-cone spectral sensitivity data after 615 nm, after which $S(\lambda)$ is so small that it can reasonably, for most purposes, be set to zero. The photopigment optical density spectra were calculated using standard formulae (see Stockman & Sharpe, 1999) assuming peak photopigment optical densities of 0.40 for $S_2(\lambda)$, and 0.50 for $L_2(\lambda)$ and $M_2(\lambda)$ and the tabulated lens and macular pigment densities for 2°.

[d] Alternative definitions of the 2° cone fundamentals in terms of the Stiles and Burch (1955) 2° CMFs, the transformations of which are not tabulated, are M: $\bar{m}_R/\bar{m}_B = 0.29089$ and $\bar{m}_G/\bar{m}_B = 12.24415$; and L: $\bar{l}_G/\bar{l}_B = 16.782165$ and $\bar{l}_R/\bar{l}_B = 4.787127$.

[e] Table 2 supercedes Table 2.1 of Stockman and Sharpe (1999), from which it differs by 0.01 log unit or less in the region 650–730 nm due to a small correction to the re-interpolation of the underlying $\bar{g}_{10}(\lambda)$ CMF (see Table 3). The M- and S-cone functions have also been renormalized.

Table 3
Stiles and Burch 10° CMFs used to calculate the cone fundamentals tabulated in Table 2 [a,b]

(λ) nm	$\bar{r}_{10}(\lambda)$	$\bar{g}_{10}(\lambda)$	$\bar{b}_{10}(\lambda)$	(λ) nm	$\bar{r}_{10}(\lambda)$	$\bar{g}_{10}(\lambda)$	$\bar{b}_{10}(\lambda)$
390	0.001500	−0.000400	0.006200	615	2.719400	0.093800	−0.001030
395	0.003800	−0.001000	0.016100	620	2.452600	0.061100	−0.000680
400	0.008900	−0.002500	0.040000	625	2.170000	0.037100	−0.000442
405	0.018800	−0.005900	0.090600	630	1.835800	0.021500	−0.000272
410	0.035000	−0.011900	0.180200	635	1.517900	0.011200	−0.000141
415	0.053100	−0.020100	0.308800	640	1.242800	0.004400	−5.49E-05
420	0.070200	−0.028900	0.467000	645	1.007000	0.000078	−2.20E-06
425	0.076300	−0.033800	0.615200	650	0.782700	−0.001368	2.37E-05
430	0.074500	−0.034900	0.763800	655	0.593400	−0.001988	2.86E-05
435	0.056100	−0.027600	0.877800	660	0.444200	−0.002168	2.61E-05
440	0.032300	−0.016900	0.975500	665	0.328300	−0.002006	2.25E-05
445	−0.004400	0.002400	1.001900	670	0.239400	−0.001642	1.82E-05
450	−0.047800	0.028300	0.999600	675	0.172200	−0.001272	1.39E-05
455	−0.097000	0.063600	0.913900	680	0.122100	−0.000947	1.03E-05
460	−0.158600	0.108200	0.829700	685	0.085300	−0.000683	7.38E-06
465	−0.223500	0.161700	0.741700	690	0.058600	−0.000478	5.22E-06
470	−0.284800	0.220100	0.613400	695	0.040800	−0.000337	3.67E-06
475	−0.334600	0.279600	0.472000	700	0.028400	−0.000235	2.56E-06
480	−0.377600	0.342800	0.349500	705	0.019700	−0.000163	1.76E-06
485	−0.413600	0.408600	0.256400	710	0.013500	−0.000111	1.20E-06
490	−0.431700	0.471600	0.181900	715	0.009240	−7.48E-05	8.17E-07
495	−0.445200	0.549100	0.130700	720	0.006380	−5.08E-05	5.55E-07
500	−0.435000	0.626000	0.091000	725	0.004410	−3.44E-05	3.75E-07
505	−0.414000	0.709700	0.058000	730	0.003070	−2.34E-05	2.54E-07
510	−0.367300	0.793500	0.035700	735	0.002140	−1.59E-05	1.71E-07
515	−0.284500	0.871500	0.020000	740	0.001490	−1.07E-05	1.16E-07
520	−0.185500	0.947700	0.009500	745	0.001050	−7.23E-06	7.85E-08
525	−0.043500	0.994500	0.000700	750	0.000739	−4.87E-06	5.31E-08
530	0.127000	1.020300	−0.004300	755	0.000523	−3.29E-06	3.60E-08
535	0.312900	1.037500	−0.006400	760	0.000372	−2.22E-06	2.44E-08
540	0.536200	1.051700	−0.008200	765	0.000265	−1.50E-06	1.65E-08
545	0.772200	1.039000	−0.009400	770	0.000190	−1.02E-06	1.12E-08
550	1.005900	1.002900	−0.009700	775	0.000136	−6.88E-07	7.53E-09
555	1.271000	0.969800	−0.009700	780	9.84E-05	−4.65E-07	5.07E-09
560	1.557400	0.916200	−0.009300	785	7.13E-05	−3.12E-07	3.40E-09
565	1.846500	0.857100	−0.008700	790	5.18E-05	−2.08E-07	2.27E-09
570	2.151100	0.782300	−0.008000	795	3.77E-05	−1.37E-07	1.50E-09
575	2.425000	0.695300	−0.007300	800	2.76E-05	−8.80E-08	9.86E-10
580	2.657400	0.596600	−0.006300	805	2.03E-05	−5.53E-08	6.39E-10
585	2.915100	0.506300	−0.005370	810	1.49E-05	−3.36E-08	4.07E-10
590	3.077900	0.420300	−0.004450	815	1.10E-05	−1.96E-08	2.53E-10
595	3.161300	0.336000	−0.003570	820	8.18E-06	−1.09E-08	1.52E-10
600	3.167300	0.259100	−0.002770	825	6.09E-06	−5.70E-09	8.64E-11
605	3.104800	0.191700	−0.002080	830	4.55E-06	−2.77E-09	4.42E-11
610	2.946200	0.136700	−0.001500	–	–	–	–

[a] The CMFs are based on Table I (5.5.4) of Wyszecki and Stiles (1982), in which they are tabulated in wavelength steps of 5 nm, and Tables 7 and 8 of Stiles and Burch (1959), in which they are tabulated in wavenumber steps of 250 or 500 cm^{-1}. At shorter wavelengths, the CMFs are the same as in Table I (5.5.4). At longer wavelengths, however, the CMFs in Table I (5.5.4) are uncorrected for rod intrusion, and are tabulated only to four decimal places, which is too imprecise to define the cone sensitivities. At longer wavelengths, therefore, we have corrected the original CMFs (Table 7 of Stiles & Burch, 1959) for rod intrusion (according to the corrections given in Table 8 of Stiles & Burch, 1959) and re-interpolated them at 5-nm intervals.

[b] It should be noted that the Stiles and Burch (1959) CMFs were based on data from 49 observers below 714.3 nm, but on data from only nine observers from 714.3 to 824.2 nm.

References

Asenjo, A. B., Rim, J., & Oprian, D. D. (1994). Molecular determinants of human red/green color discrimination. *Neuron*, *12*, 1131–1138.

Barlow, H. B. (1982). What causes trichromacy? A theoretical analysis using comb-filtered spectra. *Vision Research*, *22*, 635–643.

Baylor, D. A., Nunn, B. J., & Schnapf, J. L. (1984). The photocurrent, noise and spectral sensitivity of rods of the monkey *Macaca fascicularis*. *Journal of Physiology*, *357*, 575–607.

Baylor, D. A., Nunn, B. J., & Schnapf, J. L. (1987). Spectral sensitivity of cones of the monkey *Macaca fascicularis*. *Journal of Physiology*, *390*, 145–160.

Bone, R. A., Landrum, J. T., & Cains, A. (1992). Optical density spectra of the macular pigment in vivo and in vitro. *Vision Research*, *32*, 105–110.

Bouma, P. J. (1942). Mathematical relationship between the colour vision system of trichromats and dichromats. *Physica*, *9*, 773–784.

Bowmaker, J. K., Dartnall, H. J. A., Lythgoe, J. N., & Mollon, J. D. (1978). The visual pigments of rods and cones in the rhesus monkey *Macaca mulatta*. *Journal of Physiology*, *274*, 329–348.

Brindley, G. S. (1954). The summation areas of human colour-receptive mechanisms at increment threshold. *Journal of Physiology*, *124*, 400–408.

Brindley, G. S., Du Croz, J. J., & Rushton, W. A. H. (1966). The flicker fusion frequency of the blue-sensitive mechanism of colour vision. *Journal of Physiology*, *183*, 497–500.

Cicerone, C. M., & Nerger, J. L. (1989). The relative numbers of long-wavelength-sensitive to middle-wavelength-sensitive cones in the human fovea centralis. *Vision Research*, *29*, 115–128.

CIE (1926). Commission Internationale de l'Éclairage Proceedings, 1924. Cambridge University Press, Cambridge.

CIE (1932). Commission Internationale de l' Éclairage Proceedings, 1931. Cambridge University Press, Cambridge.

Coblentz, W. W., & Emerson, W. B. (1918). Relative sensibility of the average eye to light of different color and some practical applications. *US Bureau of Standards Bulletin*, *14*, 167.

Dartnall, H. J. A. (1953). The interpretation of spectral sensitivity curves. *British Medical Bulletin*, *9*, 24–30.

Dartnall, H. J. A., Bowmaker, J. K., & Mollon, J. D. (1983). Human visual pigments: microspectrophotometric results from the eyes of seven persons. *Proceedings of the Royal Society of London*, *B*, *220*, 115–130.

De Vries, H. (1948). The luminosity curve of the eye as determined by measurements with the flicker photometer. *Physica*, *14*, 319–348.

Eisner, A., & MacLeod, D. I. A. (1980). Blue sensitive cones do not contribute to luminance. *Journal of the Optical Society of America*, *70*, 121–123.

Eisner, A., & MacLeod, D. I. A. (1981). Flicker photometric study of chromatic adaptation: selective suppression of cone inputs by colored backgrounds. *Journal of the Optical Society of America*, *71*, 705–718.

Elenbaas, W. (1951). *The high pressure mercury vapour discharge*. Amsterdam: North-Holland Publishers.

Enoch, J. M. (1961). Nature of the transmission of energy in the retinal receptors. *Journal of the Optical Society of America*, *51*, 1122–1126.

Enoch, J. M. (1963). Optical properties of the retinal receptors. *Journal of the Optical Society of America*, *53*, 71–85.

Enoch, J. M., & Stiles, W. S. (1961). The colour change of monochromatic light with retinal angle of incidence. *Optica Acta*, *8*, 329–358.

Estévez, O. (1979). On the fundamental database of normal and dichromatic color vision. Ph.D. thesis, Amsterdam University.

Gibson, K. S., & Tyndall, E. P. T. (1923). Visibility of radiant energy. *Scientific Papers of the Bureau of Standards*, *19*, 131–191.

Guild, J. (1931). The colorimetric properties of the spectrum. *Philosophical Transactions of the Royal Society of London*, *A230*, 149–187.

Hecht, S. (1949). Brightness, visual acuity and color blindness. *Documenta Ophthalmologica*, *3*, 289–306.

Horowitz, B. R. (1981). Theoretical considerations of the retinal receptor as a waveguide. In J. M. Enoch, & F. L. Tobey, *Vertebrate photoreceptor optics* (pp. 217–300). Berlin, New York: Springer-Verlag.

Hsia, Y., & Graham, C. H. (1957). Spectral luminosity curves for protanopic, deuteranopic, and normal subjects. *Proceedings of the National Academy of Science USA*, *43*, 1011–1019.

Hyde, E. P., Forsythe, W. E., & Cady, F. E. (1918). The visibility of radiation. *Astrophysics Journal*, *48*, 65–83.

Ives, H. E. (1912). Studies in the photometry of lights of different colours. I. Spectral luminosity curves obtained by the equality of brightness photometer and flicker photometer under similar conditions. *Philosophical Magazine Series*, *6*(24), 149–188.

Judd, D. B. (1945). Standard response functions for protanopic and deuteranopic vision. *Journal of the Optical Society of America*, *35*, 199–221.

Judd, D. B. (1949). Standard response functions for protanopic and deuteranopic vision. *Journal of the Optical Society of America*, *39*, 505.

Judd, D. B. (1951). Report of U.S. Secretariat Committee on Colorimetry and Artificial Daylight, Proceedings of the Twelfth Session of the CIE, Stockholm. Bureau Central de la CIE, Paris, pp. 11.

King-Smith, P. E., & Webb, J. R. (1974). The use of photopic saturation in determining the fundamental spectral sensitivity curves. *Vision Research*, *14*, 421–429.

Knau, H., Schmidt, H.-J., Wolf, S., Wissinger, B., & Sharpe, L. T. (1999). M-cone opsin gene number and phenotype. *Investigative Ophthalmology and Visual Science* (*supplement*), *40*, S353.

König, A., & Dieterici, C. (1886). Die Grundempfindungen und ihre Intensitäts-Vertheilung im Spectrum. *Sitzungsberichte Akademie der Wissenschaften*, *Berlin*, 805–829.

Kraft, T. W., Neitz, J., & Neitz, M. (1998). Spectra of human L-cones. *Vision Research*, *38*, 3663–3670.

Lamb, T. D. (1995). Photoreceptor spectral sensitivities: common shape in the long-wavelength spectral region. *Vision Research*, *35*, 3083–3091.

Lee, J., & Stromeyer, C. F. (1989). Contribution of human short-wave cones to luminance and motion detection. *Journal of Physiology*, *413*, 563–593.

Macke, J. P., & Nathans, J. (1997). Individual variation in the size of the human red and green pigment gene array. *Investigative Ophthalmology and Visual Science*, *38*, 1040–1043.

MacLeod, D. I. A., & Boynton, R. M. (1979). Chromaticity diagram showing cone excitation by stimuli of equal luminance. *Journal of the Optical Society of America*, *69*, 1183–1186.

MacNichol, E. F. (1986). A unifying presentation of photopigment spectra. *Vision Research*, *26*, 1543–1556.

Mansfield, R. J. W. (1985). Primate photopigments and cone mechanisms. In A. Fein, & J. S. Levine, *The visual system* (pp. 89–106). New York: Alan R. Liss.

Maxwell, J. C. (1856). On the theory of colours in relation to colour-blindness. A letter to Dr G. Wilson. *Transactions of the Royal Scottish Society of Arts*, *4*, 394–400.

Maxwell, J. C. (1860). On the theory of compound colours and the relations of the colours of the spectrum. *Philosophical Transactions of the Royal Society of London*, *150*, 57–84.

Merbs, S. L., & Nathans, J. (1992). Absorption spectra of the hybrid pigments responsible for anomalous color vision. *Science*, *258*, 464–466.

Nathans, J., Merbs, S. L., Sung, C.-H., Weitz, C. J., & Wang, Y. (1992). Molecular genetics of human visual pigments. *Annual Review of Genetics*, *26*, 401–422.

Nathans, J., Piantanida, T. P., Eddy, R. L., Shows, T. B., & Hogness, S. G. (1986a). Molecular genetics of inherited variation in human color vision. *Science*, *232*, 203–210.

Nathans, J., Thomas, D., & Hogness, S. G. (1986b). Molecular genetics of human color vision: The genes encoding blue, green and red pigments. *Science*, *232*, 193–202.

Neitz, M., & Neitz, J. (1998). Molecular genetics and the biological basis of color vision. In W. G. K. Backhaus, R. Kliegl, & J. S. Werner, *Color vision: perspectives from different disciplines* (pp. 101–119). Berlin: Walter de Gruyter.

Nunn, B. J., Schnapf, J. L., & Baylor, D. A. (1984). Spectral sensitivity of single cones in the retina of *Macaca fascicularis*. *Nature*, *309*, 264–266.

Pitt, F. H. G. (1935). Characteristics of dichromatic vision. Medical Research Council Special Report Series, No. 200. His Majesty's Stationery Office, London.

Pokorny, J., & Smith, V. C. (1993). Monochromatic tritan metamers. *Optical Society of America Technical Digest*, *16*, 84.

Polyak, S. L. (1941). *The retina*. Chicago: University of Chicago.

Rayleigh, L. (1881). Experiments on colour. *Nature*, *25*, 64–66.

Schnapf, J. L., Kraft, T. W., & Baylor, D. A. (1987). Spectral sensitivity of human cone photoreceptors. *Nature*, *325*, 439–441.

Sharpe, L. T., Stockman, A., Jägle, H., Knau, H., Klausen, G., Reitner, A., & Nathans, J. (1998a). Red, green, and red–green hybrid photopigments in the human retina: correlations between deduced protein sequences and psychophysically-measured spectral sensitivities. *Journal of Neuroscience*, *18*, 10053–10069.

Sharpe, L. T., Stockman, A., Knau, H., & Jägle, H. (1998b). Macular pigment densities derived from central and peripheral spectral sensitivity differences. *Vision Research*, *38*, 3233–3239.

Sharpe, L. T., Stockman, A., Jägle, H., Knau, H., & Nathans, J. (1999a). L, M and L–M hybrid cone photopigments in man: deriving λ_{max} from flicker photometric spectral sensitivities. *Vision Research*, *39*, 3513–3525.

Sharpe, L. T., Stockman, A., Jägle, H., & Nathans, J. (1999b). Opsin genes, cone photopigments, color vision and colorblindness. In K. Gegenfurtner, & L. T. Sharpe, *Color vision: from genes to perception* (pp. 3–51). Cambridge: Cambridge University Press.

Smith, V. C., & Pokorny, J. (1975). Spectral sensitivity of the foveal-cone photopigments between 400 and 500 nm. *Vision Research*, *15*, 161–171.

Snodderly, D. M., Brown, P. K., Delori, F. C., & Auran, J. D. (1984). The macular pigment. I. Absorbance spectra, localization, and discrimination from other yellow pigments in primate retina. *Investigative Ophthalmology and Visual Science*, *25*, 660–673.

Snyder, A. W. (1975). Photoreceptor optics — theoretical principles. In A. W. Snyder, & R. Menzel, *Photoreceptor optics* (pp. 38–55). Berlin, Heidelburg, New York: Springer-Verlag.

Speranskaya, N. I. (1959). Determination of spectrum color co-ordinates for twenty-seven normal observers. *Optics and Spectroscopy*, *7*, 424–428.

Sperling, H. G. (1958). An experimental investigation of the relationship between colour mixture and luminous efficiency. In *Visual-problems of colour*, vol. 1 (pp. 249–277). London: Her Majesty's Stationery Office.

Stiles, W. S. (1939). The directional sensitivity of the retina and the spectral sensitivity of the rods and cones. *Proceedings of the Royal Society of London*, *B127*, 64–105.

Stiles, W. S. (1949). Incremental thresholds and the mechanisms of colour vision. *Documenta Ophthalmologica*, *3*, 138–163.

Stiles, W. S. (1955). Interim report to the Commission Internationale de l'Éclairage Zurich, 1955, on the National Physical Laboratory's investigation of colour-matching (1955) with an appendix by W. S. Stiles & J. M. Burch. *Optica Acta*, *2*, 168–181.

Stiles, W. S. (1964). Foveal threshold sensitivity on fields of different colors. *Science*, *145*, 1016–1018.

Stiles, W. S. (1978). *Mechanisms of colour vision*. London: Academic.

Stiles, W. S., & Burch, J. M. (1959). NPL colour-matching investigation: final report (1958). *Optica Acta*, *6*, 1–26.

Stockman, A., MacLeod, D. I. A., & DePriest, D. D. (1987). An inverted S-cone input to the luminance channel: evidence for two processes in S-cone flicker detection. *Investigative Ophthalmology and Visual Science* (*supplement*), *28*, 92.

Stockman, A., MacLeod, D. I. A., & DePriest, D. D. (1991). The temporal properties of the human short-wave photoreceptors and their associated pathways. *Vision Research*, *31*, 189–208.

Stockman, A., MacLeod, D. I. A., & Johnson, N. E. (1993a). Spectral sensitivities of the human cones. *Journal of the Optical Society of America A*, *10*, 2491–2521.

Stockman, A., MacLeod, D. I. A., & Vivien, J. A. (1993b). Isolation of the middle- and long-wavelength sensitive cones in normal trichromats. *Journal of the Optical Society of America A*, *10*, 2471–2490.

Stockman, A., & Mollon, J. D. (1986). The spectral sensitivities of the middle- and long-wavelength cones: an extension of the two-colour threshold technique of W. S. Stiles. *Perception*, *15*, 729–754.

Stockman, A., & Sharpe, L. T. (1999). Cone spectral sensitivities and color matching. In K. Gegenfurtner, & L. T. Sharpe, *Color vision: from genes to perception* (pp. 53–87). Cambridge: Cambridge University Press.

Stockman, A., & Sharpe, L. T. (2000). Tritanopic color matches and the middle- and long-wavelength-sensitive cone spectral sensitivities. *Vision Research*, *40*, 1739–1750.

Stockman, A., Sharpe, L. T., & Fach, C. C. (1999). The spectral sensitivity of the human short-wavelength cones. *Vision Research*, *39*, 2901–2927.

Stockman, A., Sharpe, L. T., Merbs, S., & Nathans, J. (2000). Spectral sensitivities of human cone visual pigments determined in vivo and in vitro. In K. Palczewski, *Vertebrate phototransduction and the visual cycle*, *Part B*, *Methods in Enzymology*, *Vol. 316* (pp. 626–650). New York: Academic Press.

van Norren, D., & Vos, J. J. (1974). Spectral transmission of the human ocular media. *Vision Research*, *14*, 1237–1244.

Verdon, W., & Adams, A. J. (1987). Short-wavelength sensitive cones do not contribute to mesopic luminosity. *Journal of the Optical Society of America A*, *4*, 91–95.

Vimal, R. L. P., Smith, V. C., Pokorny, J., & Shevell, S. K. (1989). Foveal-cone thresholds. *Vision Research*, *29*, 61–78.

Vos, J. J. (1972). Literature review of human macular absorption in the visible and its consequences for the cone receptor primaries. Soesterberg, The Netherlands: Netherlands Organization for applied scientific research, Institute for Perception.

Vos, J. J. (1978). Colorimetric and photometric properties of a 2-deg fundamental observer. *Color Research and Application*, *3*, 125–128.

Vos, J. J., Estévez, O., & Walraven, P. L. (1990). Improved color fundamentals offer a new view on photometric additivity. *Vision Research*, *30*, 936–943.

Vos, J. J., & Walraven, P. L. (1971). On the derivation of the foveal receptor primaries. *Vision Research*, *11*, 799–818.

Wagner, G., & Boynton, R. M. (1972). Comparison of four methods of heterochromatic photometry. *Journal of the Optical Society of America*, *62*, 1508–1515.

Wald, G. (1964). The receptors of human color vision. *Science*, *145*, 1007–1016.

Winderickx, J., Battisti, L., Hibiya, Y., Motulsky, A. G., & Deeb, S. S. (1993). Haplotype diversity in the human red and green opsin genes: evidence for frequent sequence exchange in exon 3. *Human Molecular Genetics*, *2*, 1413–1421.

Wolf, S., Sharpe, L. T., Schmidt, H.-J. A., Knau, H., Weitz, S., Kioschis, P., Poustka, A., Zrenner, E., Lichter, P., & Wissinger, B. H. (1999). Direct visual resolution of gene copy number in the human photopigment gene array. *Investigative Opthalmology & Visual Science*, *40*, 1585–1589.

Wright, W. D. (1928). A re-determination of the trichromatic coefficients of the spectral colours. *Transactions of the Optical Society*, *30*, 141–164.

Wright, W. D. (1952). The characteristics of tritanopia. *Journal of the Optical Society of America*, *42*, 509–521.

Wyszecki, G., & Stiles, W. S. (1967). *Color science: concepts and methods*, *quantitative data and formulae* (1st ed.). New York: Wiley.

Wyszecki, G., & Stiles, W. S. (1982). *Color science: concepts and methods*, *quantitative data and formulae* (2nd ed.). New York: Wiley.